

Supporting Info - On the Dynamic Nature of Mo sites for Methane Dehydroaromatization

Ina Vollmer¹, Bart van der Linden¹, Samy Ould-Chikh², Antonio Aguilar-Tapia⁴, Irina Yarulina^{1,2}, Edy Abou-Hamad³, Yuri G. Sneider⁵, Alma I. Olivos Suarez¹, Jean-Louis Hazemann⁴, Freek Kapteijn¹ and Jorge Gascon^{1,2}

¹ Catalysis Engineering, Chemical Engineering Department Delft University of Technology, Van der Maasweg 9, 2629 HZ Delft, The Netherlands.

² King Abdullah University of Science and Technology, KAUST Catalysis Center, Advanced Catalytic Materials, Thuwal 23955, Saudi Arabia

³ King Abdullah University of Science and Technology, Core Labs, Thuwal 23955, Saudi Arabia

⁴ Inst. Néel, UPR 2940 CNRS - Univ. Grenoble Alpes, F-38000 Grenoble, France

⁵ Dipartimento di Ingegneria Chimica Materiali Ambiente, Sapienza Università di Roma, Via Eudossiana 18, 00184 Roma, Italia

Contents

Catalyst Synthesis.....	2
N ₂ Adsorption.....	31
PXRD.....	32
CO carburization.....	2
Temperature Programmed Carburization (TPC)	2
Quantification	4
Temperature Programmed Oxidation (TPO).....	22
¹³ C MAS NMR.....	6
Deconvolution of ¹³ C NMR spectra	21
Activity Relationships	22
Catalytic performance	25
X-ray Absorption spectroscopy (XAS).....	6
Pulsing CH ₄	6
Effect of CO-treatment	7
Effect of H ₂ -treatment.....	10
CH ₄ pulsing using labelled molecules – benzene control experiments	25
CH ₄ pulsing using labelled molecules - ethylene and ethane.....	29
Gas chromatography-mass spectrometry (GC-MS) analysis of the collected liquid products	29
References.....	33

Catalyst Synthesis

Catalyst synthesis. 1, 2 and 5 wt.% of molybdenum (Mo) were introduced into a commercial zeolite with Si/Al = 13 (Südchemie), denoted as $y\text{MoHZ-13}$, where y denotes the wt.% of Mo introduced. $(\text{NH}_4)_6\text{Mo}_7\text{O}_{24}\cdot 4\text{H}_2\text{O}$ was dissolved in 210 μl of de-ionized water per gram of catalyst and introduced dropwise to the ammonia form of the zeolite dehydrated at 150 °C in vacuum. After mixing solution and zeolite well, the sample was dried overnight at 80 °C and subsequently calcined at 550 °C for 7 h with a heating rate of 2 °C/min. Another sample denoted as 2MoS was produced for ^{13}C NMR measurements introducing 2 wt.% of Mo into silicalite-1 using the same method as described above. Silicalite-1 was synthesized mixing 25.6 g of TPAOH with 30.0 g of distilled water, after which 36.9 g of TEOS was added dropwise to the solution. The obtained mixture is aged at room temperature overnight. Afterwards the mixture was transferred into autoclaves to perform further crystallization at 150 °C for 10 days. After cooling down, the product was collected by filtration and washing, and dried in air overnight. The dried product was calcined at 550 °C for 5 h (2 °C/min) to remove the residue template.^[1]

CO carburization

CO carburization was performed on a custom-made setup, where a 30 ml/min flow of 2.5% CO in He was continuously fed to the reactor. Effluent gasses were analyzed by a quadrupole mass spectrometer (Balzers) connected on-line with the reactor. Mass Spectra were recorded in multiple ion detection (MID) mode using a channeltron detector. Quantification of CO and CO₂ was achieved by calibrating signals with calcium oxalate.^[2] Signals were normalized with the signal of He and the fragmentation contribution of CO₂ $m/z = 44$ was subtracted from $m/z = 28$. The catalyst was pretreated at 350 °C in He overnight to desorb any adsorbed gasses from the pores of the zeolite.

Temperature Programmed Carburization (TPC)

During Temperature Programmed Carburization (TPC), CO consumption and CO₂ production were monitored using in one case labelled carbon, ^{13}CO , and in another labelled oxygen, C^{18}O . The results from carburization with ^{13}CO are shown in Figure 1, while the results for C^{18}O are shown in Figure S1. Both experiments are in good agreement (Figure S2), demonstrating the good reproducibility of the experiment. Further, it can be concluded from Figure S1 that the extent of carbon deposition due to the reverse Boudouard reaction is negligible as this would lead to the formation of C^{18}O_2 , which is only observed in very small amounts. Figure S1 shows the net consumption of C^{18}O , which was calculated by adding the signals for CO and C^{18}O shown in Figure S3. Large amounts of C^{18}O are 'consumed' while CO is 'produced', attributed to a high degree of exchange of unlabelled framework oxygen with labelled oxygen from C^{18}O . To the best of our knowledge, this was not reported previously with CO, but Voskoboinikov *et. al.*^[3] as well as Valyon *et. al.*^[4] observed an exchange of $^{18}\text{O}_2$ with framework oxygen for an iron on ZSM-5 catalyst.

To explore whether a similar extent of exchange of framework oxygen occurs without the presence of Mo, a bare zeolite HZ-13 was exposed to the same treatment in ^{18}CO . As can be seen in Figure S3 an extensive exchange is observed in this case as well, without any net consumption of CO or production of CO_2 . Quantification (see section “Quantification”) of C^{18}O consumed and CO produced shows that 12 mol% of framework O is replaced by ^{18}O in the case of 2MoHZ-13 and 25 mol% in when no Mo is present (HZ-13).

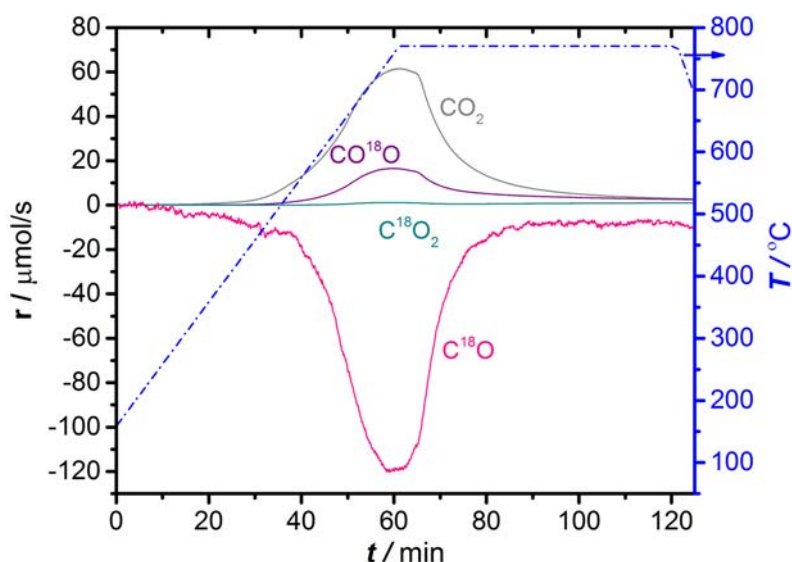


Figure S1: Net C^{18}O (sum of C^{18}O and CO signals) consumption and simultaneous CO_2 , C^{18}O_2 and CO^{18}O production in TPC of 300 mg 2MoHZ-13 with 30 ml/min, 2.5% C^{18}O in He. The temperature was increased to 780 °C at a rate of 10 °C/min (right axis).

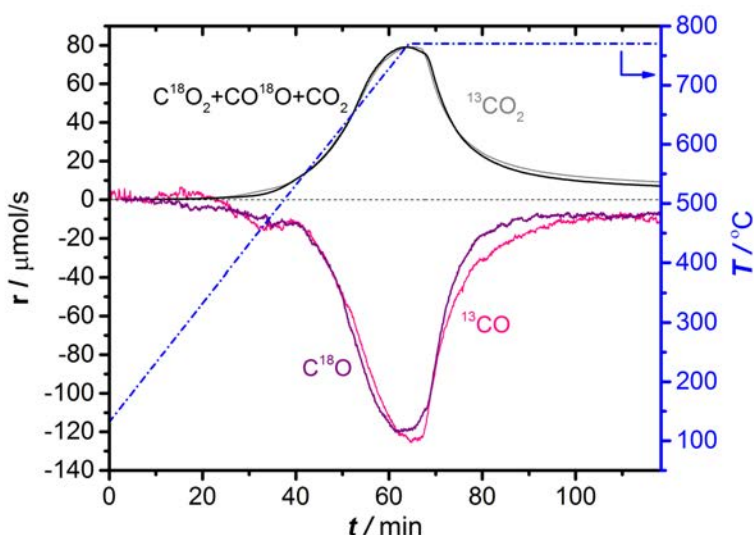


Figure S2: ^{13}CO or C^{18}O consumption and simultaneous $^{13}\text{CO}_2$ or CO_2 , C^{18}O_2 and CO^{18}O production in TPC of 2MoHZ-13 with 30 ml/min, 2.5% ^{13}CO or C^{18}O in He. The temperature was increased to 780 °C at a rate of 10 °C/min (right axis).

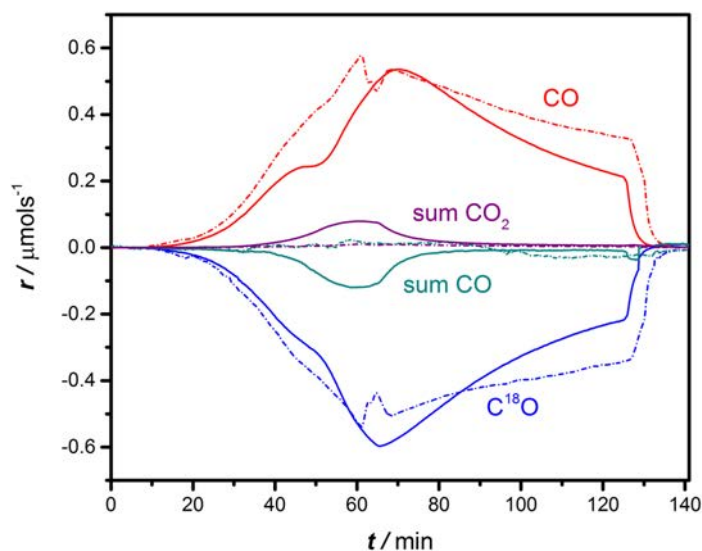


Figure S3: $C^{18}O$ consumption, CO production and net CO consumption as well as net CO_2 production for carburization of 2MoHZ-13 (solid lines) and HZ-13 (dotted lines). 300 mg catalyst was treated with 30 ml/min, 2.5% $C^{18}O$ in He. The temperature was increased to 780 °C at a rate of 10 °C/min.

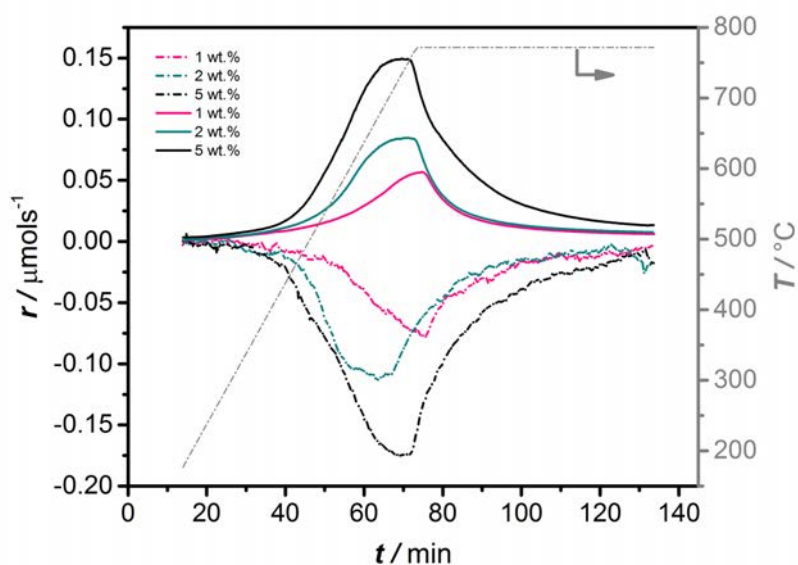
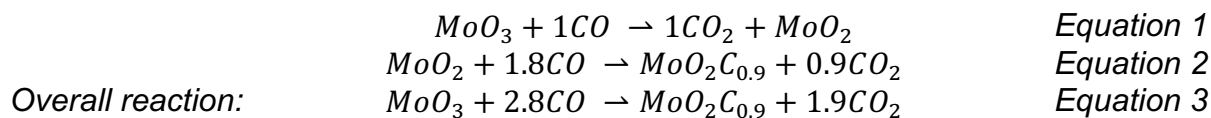


Figure S4: CO (dashed lines) and CO_2 (solid lines) evolution for 1, 2 and 5MoHZ-13, during TPC with 30 ml/min of 2.5% CO in He heating to 780 °C with 10 °C/min.

Quantification

We arrive at an oxygen to molybdenum ratio of $\frac{O}{Mo} = 1.09 \pm 0.15$ and a carbon to molybdenum ratio of $\frac{C}{Mo} = 0.90 \pm 0.15$ based on CO uptake and CO_2 calculated from Figure 1 using equations 4, 6, 8-10 and 14-15. It can be seen that, even with a maximum error, still only 1.24 oxygen is removed per molybdenum, which means that oxygen is still at the Mo site, if the initial stoichiometry of the Mo oxide is at least

MoO₂. We tentatively propose Equations 1-3, assuming an initial stoichiometry of MoO₃.



To estimate the accuracy of these results an error analysis was performed taking into account the errors arising from the necessary corrections due to fragmentation of CO₂ into CO, baseline corrections and calibration factors. All constants used for the corrections are listed in Table S1.

Table S1: List of constants used for the quantification of results shown in Figure 1 and their estimated errors.

Constant	Value and error
Factor for fragmentation of CO ₂	$\alpha = 0.25 \pm 0.07$
Calibration factor CO	$K_{CO} = 24.09 \pm 0.11 \text{ } \mu\text{mol/area}$
Calibration factor CO ₂	$K_{CO_2} = 26.08 \pm 0.33 \text{ } \mu\text{mol/area}$
Baseline correction $a + b * t$ for CO	$a_{CO} = 0.296 \pm 0.001 \text{ } 1/\text{s}$
Baseline correction $a + b * t$ for CO	$b_{CO} = (4.93 \pm 4.93) * 10^{-8} 1/\text{s}^2$
Baseline correction $a + b * t$ for CO ₂	$a_{CO_2} = (4.81 \pm 0.467) * 10^{-5} \text{ } 1/\text{s}$

Molar ratio carbon to molybdenum:	$\frac{C}{Mo} = \frac{A_{CO} + A_{CO_2}}{A_{Mo}}$	Equation 4
And associated error:	$\delta\left(\frac{C}{Mo}\right) = \frac{\delta C}{Mo} = \frac{\sqrt{\delta A_{CO}^2 + \delta A_{CO_2}^2}}{A_{Mo}}$	Equation 5
Molar ratio oxygen to molybdenum:	$\frac{O}{Mo} = \frac{A_{CO} + 2 * A_{CO_2}}{A_{Mo}}$	Equation 6
And associated error:	$\delta\left(\frac{O}{Mo}\right) = \frac{\delta O}{Mo} = \frac{\sqrt{\delta A_{CO}^2 + \delta 2A_{CO_2}^2}}{A_{Mo}}$	Equation 7
Total molar amount of CO consumed, with Δt the time step in the measurement, which is constant and can be taken in front of the sum.	$A_{CO} = K_{CO} \sum_0^{t_{end}} r_{CO}(t)\Delta t = K_{CO}\Delta t \sum_0^{t_{end}} r_{CO}(t)$	Equation 8
With $r_{CO}(t)$, the rate of CO consumption with correction for fragmentation of CO ₂ into CO with factor α determined by prior calibration.	$r_{CO}(t) = \frac{I_{CO}(t)}{I_{He}(t)} - \alpha \frac{I_{CO_2}(t)}{I_{He}(t)} - \text{baseline, CO}(t)$	Equation 9

$I_{CO}(t), I_{He}(t)$ and $I_{CO_2}(t)$ [A] are the MS signals for CO, He and CO ₂ respectively		
The sum over $r_{CO}(t)$ then becomes:	$\sum_0^{t_{end}} r_{CO}(t) = \sum_0^{t_{end}} \frac{I_{CO}(t)}{I_{He}(t)} - \alpha \sum_0^{t_{end}} \frac{I_{CO_2}(t)}{I_{He}(t)} - \sum_0^{t_{end}} baseline, CO(t)$	Equation 10
And the associated error arises from the correction due to fragmentation of CO ₂ and the baseline correction and can be written as:	$\delta\left(\sum_0^{t_{end}} r_{CO}(t)\right) = \sqrt{\left(\delta\alpha \sum_0^{t_{end}} \frac{I_{CO_2}(t)}{I_{He}(t)}\right)^2 + \left(\delta\left(\sum_0^{t_{end}} baseline, CO(t)\right)\right)^2}$	Equation 11
Where the error associated with the baseline is estimated like this:	$\delta\left(\sum_0^{t_{end}} baseline, CO(t)\right) = \sqrt{\sum_0^{t_{end}} \delta a_{CO}^2 + \sum_0^{t_{end}} t \delta b_{CO}^2}$	Equation 12
The relative error of A_{CO} is written as:	$\frac{\delta A_{CO}}{ A_{CO} } = \sqrt{\left(\frac{\delta K_{CO}}{K_{CO}}\right)^2 + \left(\frac{\delta\left(\sum_0^{t_{end}} r_{CO}(t)\right)}{\sum_0^{t_{end}} r_{CO}(t)}\right)^2}$	Equation 13
Total molar amount of CO ₂ consumed.	$A_{CO_2} = K_{CO_2} \sum_0^{t_{end}} r_{CO_2}(t) \Delta t = K_{CO_2} \Delta t \sum_0^{t_{end}} r_{CO_2}(t)$	Equation 14
Where $r_{CO_2}(t)$, the rate of CO consumption is defined as	$r_{CO_2}(t) = \frac{I_{CO_2}(t)}{I_{He}(t)} - baseline, CO_2(t)$	Equation 15
The associated error only arises from the baseline correction:	$\begin{aligned} \delta\left(\sum_0^{t_{end}} r_{CO_2}(t)\right) &= \delta\left(\sum_0^{t_{end}} baseline, CO_2(t)\right) \\ &= \sqrt{\sum_0^{t_{end}} \delta a_{CO_2}^2 + \sum_0^{t_{end}} t \delta b_{CO_2}^2} \\ &= \sqrt{t_{end}} * \delta a_{CO_2} \end{aligned}$	Equation 16
The relative error of A_{CO_2} becomes:	$\frac{\delta A_{CO_2}}{ A_{CO_2} } = \sqrt{\left(\frac{\delta K_{CO_2}}{K_{CO_2}}\right)^2 + \left(\frac{\delta\left(\sum_0^{t_{end}} r_{CO_2}(t)\right)}{\sum_0^{t_{end}} r_{CO_2}(t)}\right)^2}$	Equation 17

Pulsing CH₄

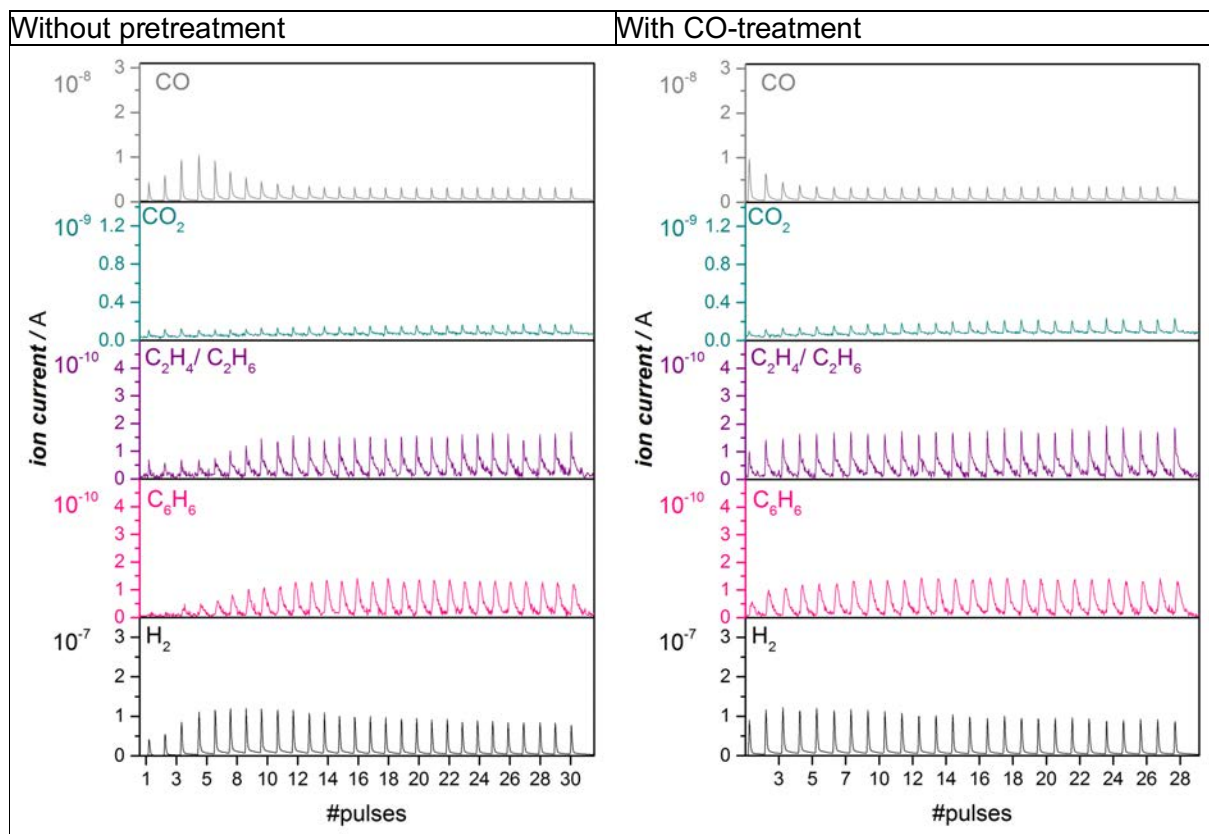
CH₄ pulsing Experiments were performed on the same setup as CO carburization and H₂-reduction. It was equipped with an injection loop in the feed line kept at atmospheric pressure, injecting 223 μmol by switching a multi-position valve to the reactor. The loop was refilled every 200 s into 30 ml/min flow of He. 300 mg Catalyst was pelletized and sieved to 212 to 425 μm particles and filled in a quartz tube with a 6 mm inner diameter.

Effect of CO-treatment

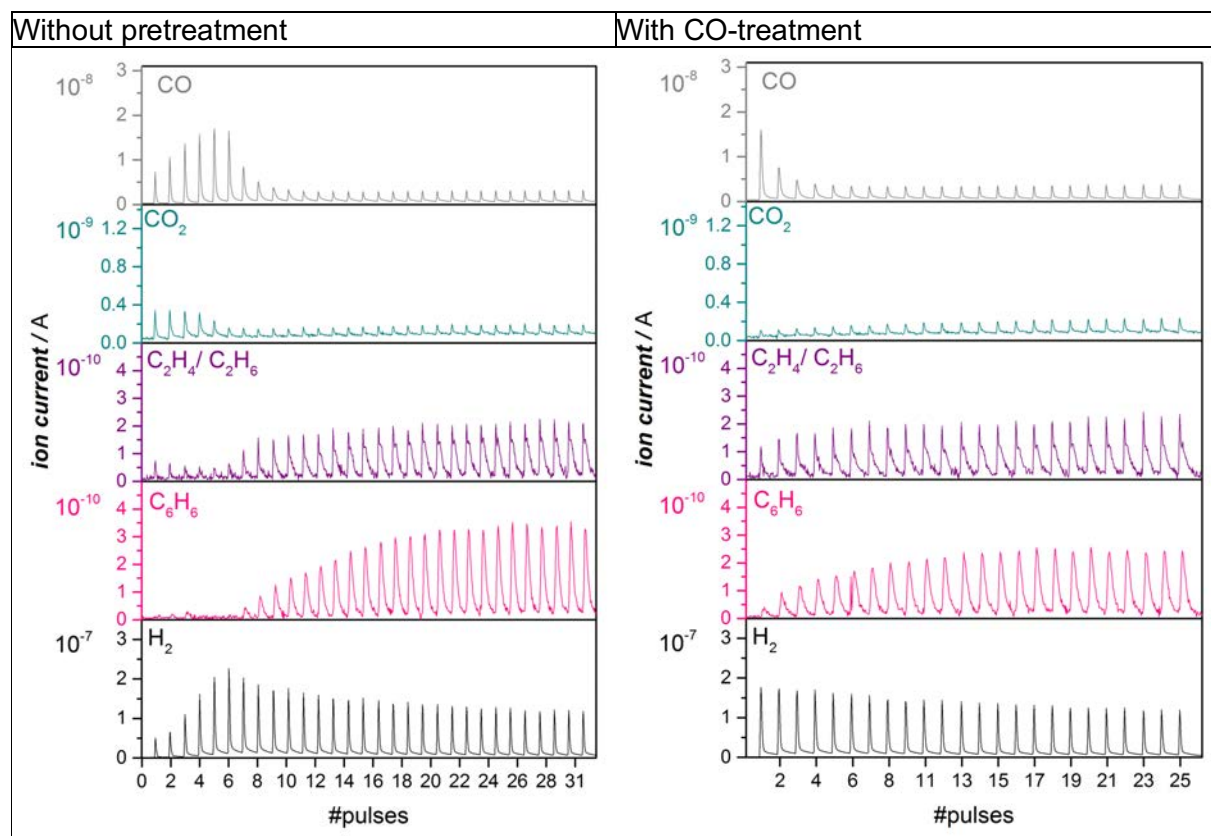
CO carburization was performed as described in section "CO carburization". No corrections for fragmentation were applied in the m/z data given in Figure S5. It can be seen that the 'CO'-signal stays high throughout the experiment even after the induction period is completed. Next to a general higher background level at $m/z = 28$ in the MS this is attributed to a pressure pulse upon injection of the 5 ml pulse of CH_4 into the continuous flow of 30 ml/min He, resulting in apparent 'CO' pulses. Further, the fragmentation of the products ethylene and ethane may also contribute to $m/z = 28$ to some extent. This is evident when comparing the presented pulse experiments with a blank, where CH_4 is sent to an empty reactor at RT. Figure S8A compares the $m/z = 28$ signal of the blank with pulses 16 to 19 of the pulsing experiment over untreated 1MoHZ-13, while Figure S8B presents all signals corresponding to ethylene and ethane that were measured in our experiments, namely $m/z = 27, 28$ and 30 , where $m/z = 28$ was corrected by subtracting the signal during the blank experiment. Signals $m/z = 27$ and 30 did not show any increase in signal during pulsing in the blank experiment as their background is nihil. Figure S8B represents the typical fragmentation pattern of a mixture of ethylene and ethane.^[5] For more detailed analysis refer to section "ethylene and ethane".

Also for the $m/z = 44$ signal (' CO_2 ') the increasing background during the experiment results in contributions from pressure pulses upon methane injection. The $m/z = 44$ is part of the fragmentation pattern of any other products observed, naphthalene, benzene, toluene, ethylene and ethane.

1MoHZ-13



2MoHZ-13



5MoHZ-13

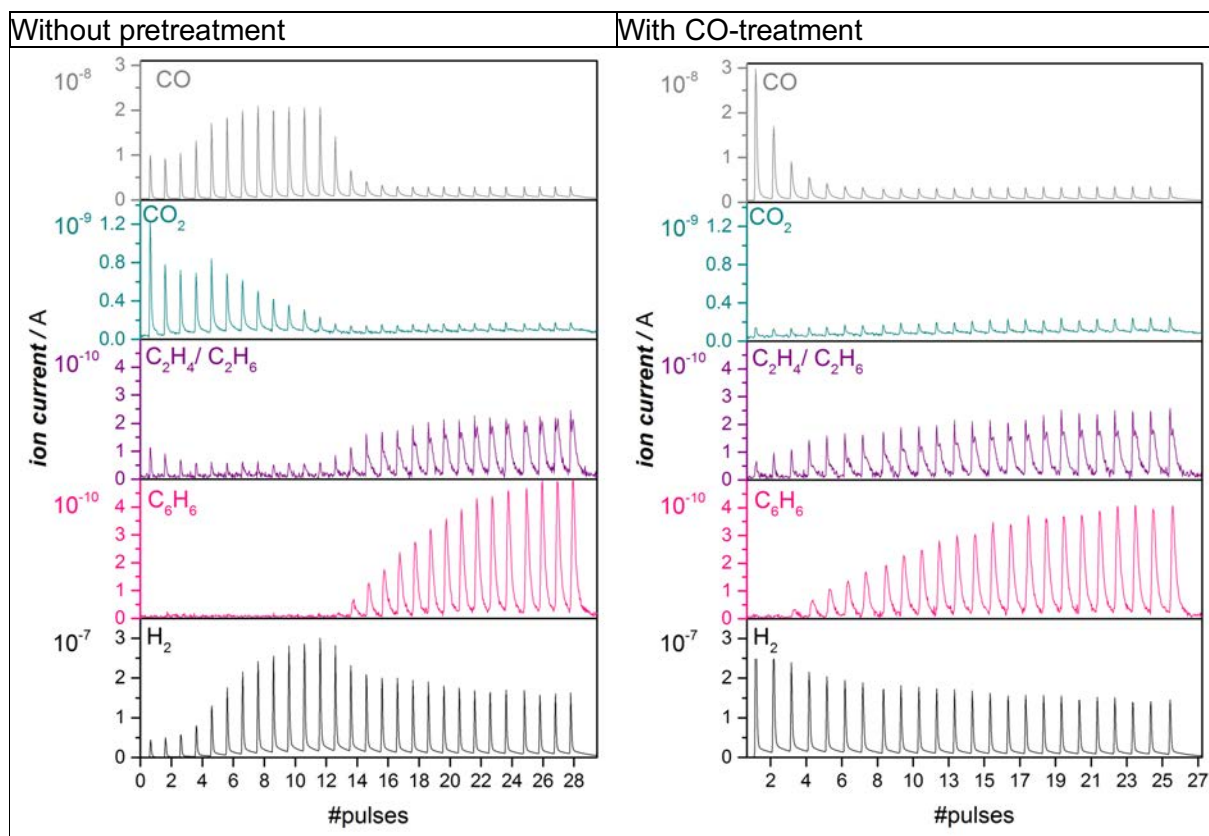


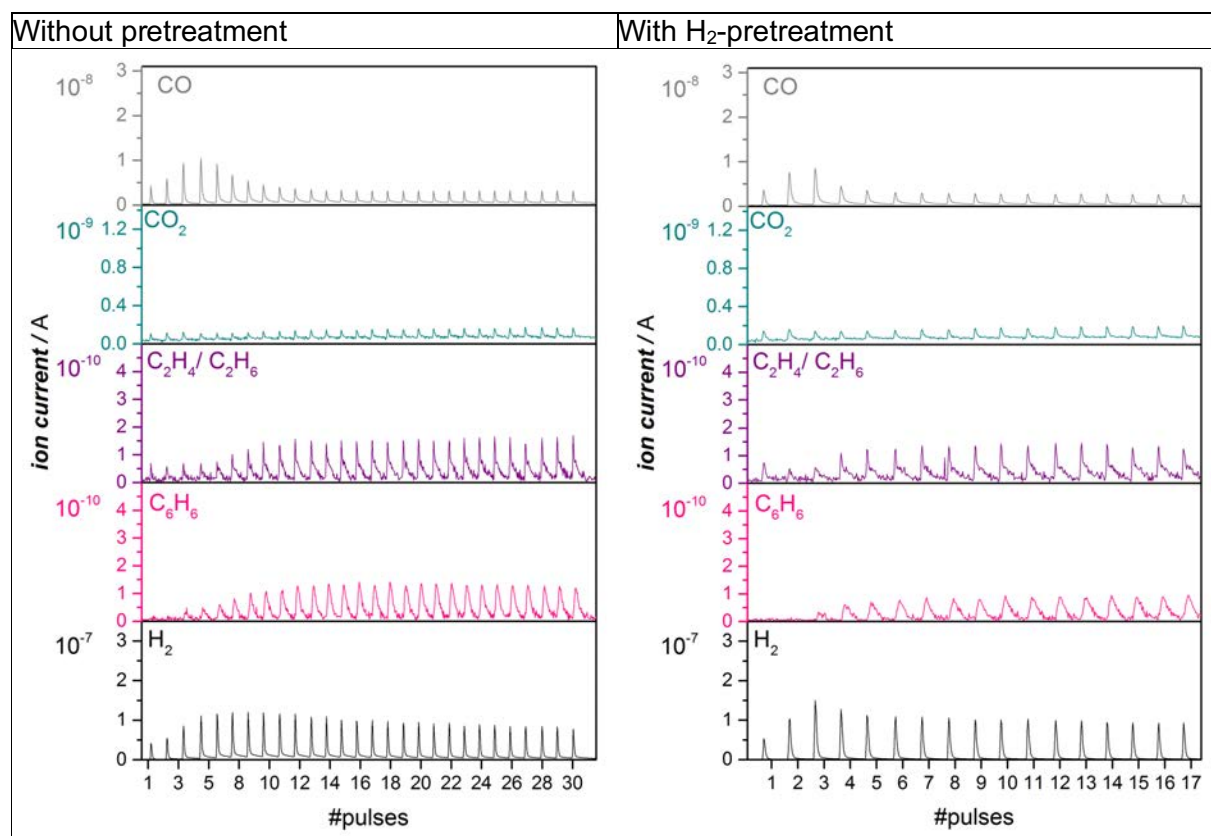
Figure S5: Ion current for CO, C₂H₄/C₂H₆, CO₂, C₆H₆ and H₂ ($m/z = 28, 27, 44, 78, 2$) during consecutive pulsing of 223 μmol CH₄ at 700 °C to 300 mg untreated catalyst (left column) and a catalyst pre-carburized with a 30 ml/min flow of 2.5% CO in He at 780 °C for 1 h (right column). From top to bottom 1, 2 and 5 wt.% MoHZ-13 samples.

Effect of H₂-treatment

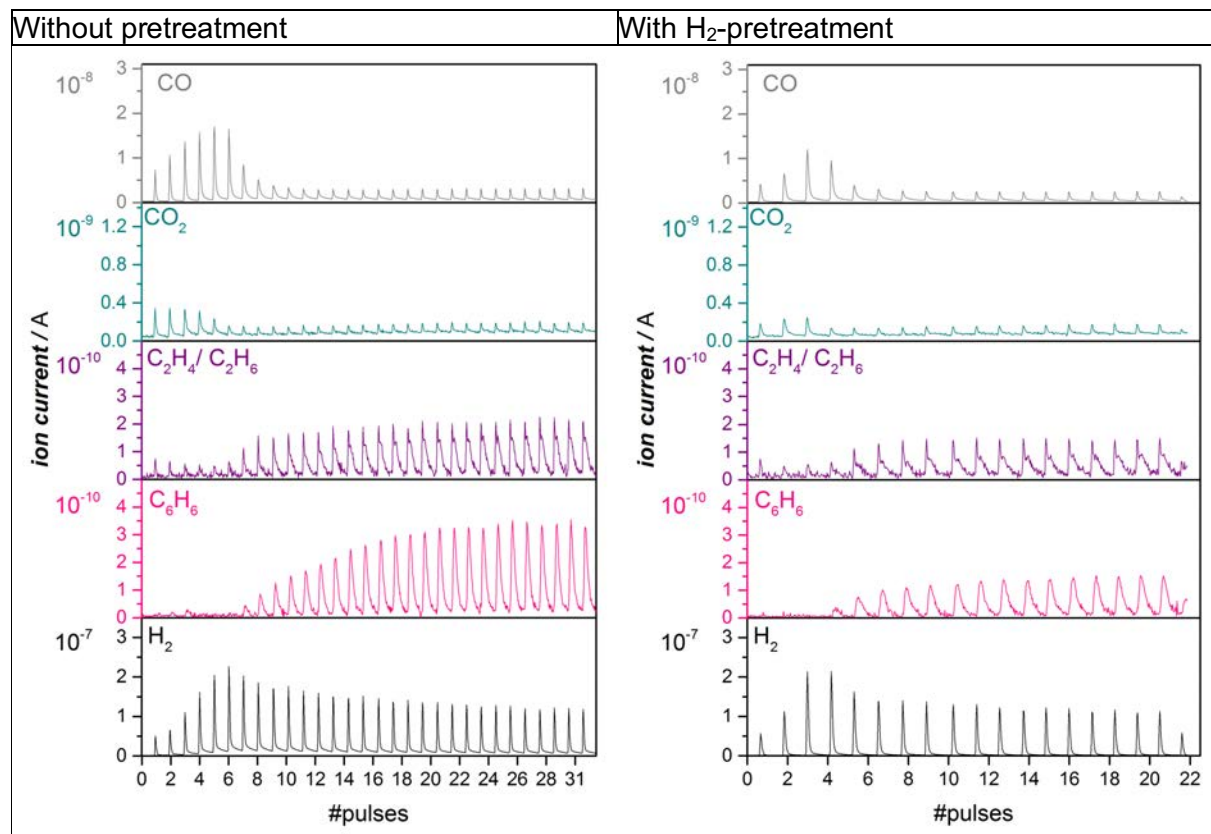
Another reduction treatment was performed to see whether a merely reduced Mo is sufficient to activate methane during consecutive pulsing of CH₄ described above. During this reduction treatment, a flow of 30 ml/min of 5% H₂ in Helium was fed to the reactor at atmospheric pressure, kept at 700 °C for 3 h, after heating at 10 °C/min. The catalyst was pretreated at 350 °C in He overnight to desorb any gasses from the zeolite. No corrections for fragmentation were applied in the *m/z* data given in Figure S6.

The results in Figure S6 show that the activation period is somewhat reduced for 5MoHZ-13 and 2MoHZ-13, but not for 1MoHZ-13. The level of benzene production seems to be lower after the H₂ treatment indicating that this treatment creates an active site that differs from the one produced at reaction conditions. The typical maximum in H₂ production right before the onset of benzene production is still observed for all three Mo loadings.

1MoHZ-13



2MHz-13



5MoHZ-13

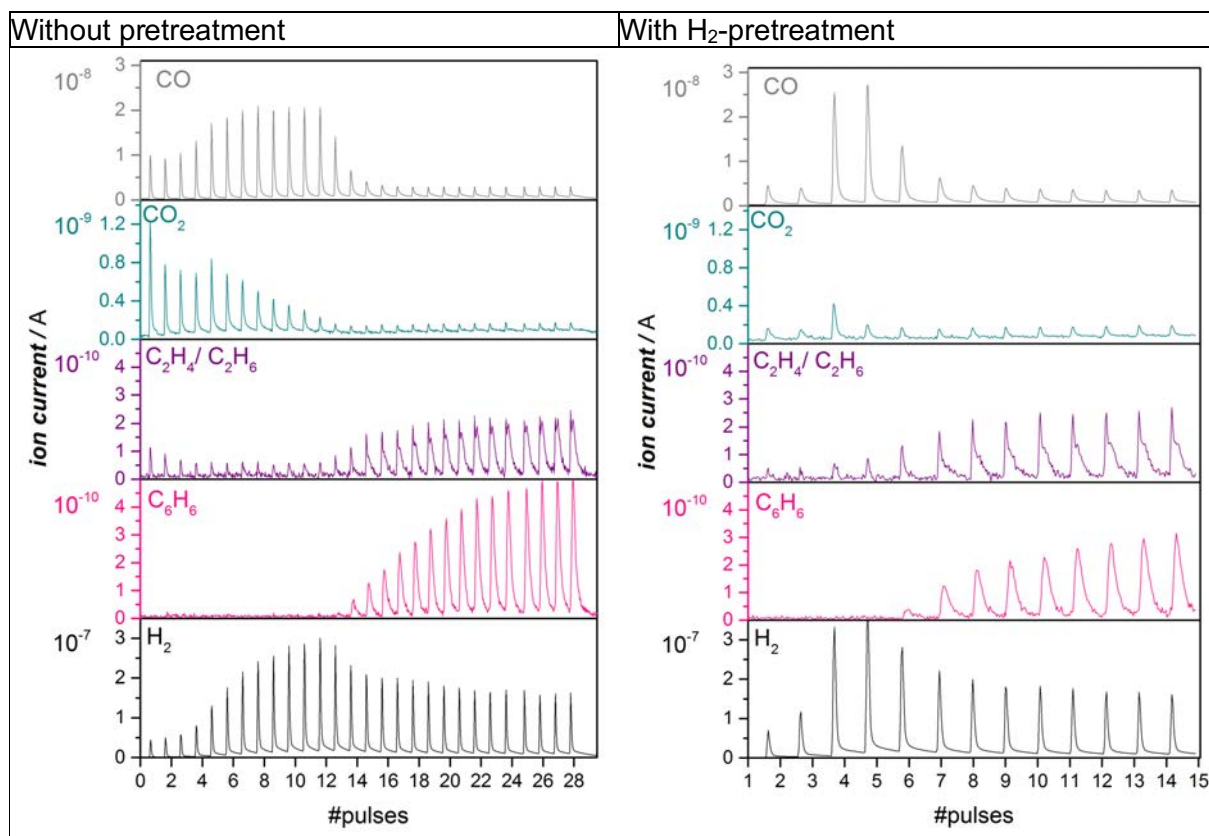


Figure S6: Ion current for CO, C₂H₄/C₂H₆, CO₂, C₆H₆ and H₂ ($m/z = 28, 27, 44, 78, 2$) during consecutive pulsing of 223 μmol of CH₄ at 700 °C to 300 mg untreated catalyst (left column) and a catalyst pre-reduced with a 30 ml/min flow of 5% H₂ in He at 700 °C for 3 h (right column). From top to bottom 1, 2 and 5 wt.% Mo/HZ-13 samples.

To test, whether a higher temperature of H₂-reduction can lead to a shortening of the induction period, sample 1MoHZ-13 was additionally reduced at 810 °C. The result from the pulsing experiment performed on a sample reduced at 810 °C is shown in Figure S7. Benzene is only observed after 3 pulses of methane have been sent to the catalyst. It can be concluded that no further reduction is observed when increasing the H₂-reduction temperature to 810 °C.

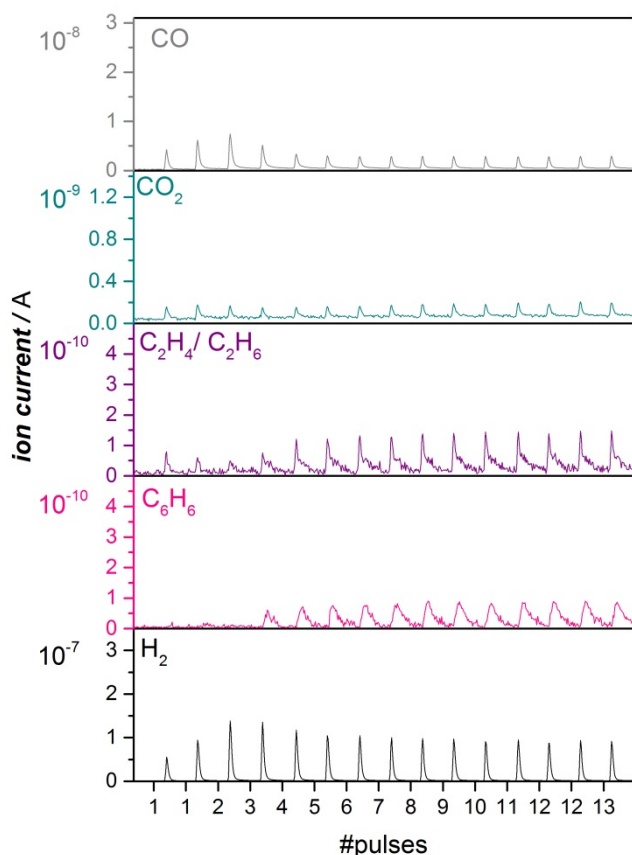


Figure S7: Ion current for CO, C₂H₄/C₂H₆, CO₂, C₆H₆ and H₂ ($m/z = 28, 27, 44, 78, 2$) during consecutive pulsing of 223 μmol of CH₄ at 700 °C to 300 mg 1MoHZ-13 pre-reduced in a 30 ml/min flow of 5% H₂ in He at 810 °C for 1 h.

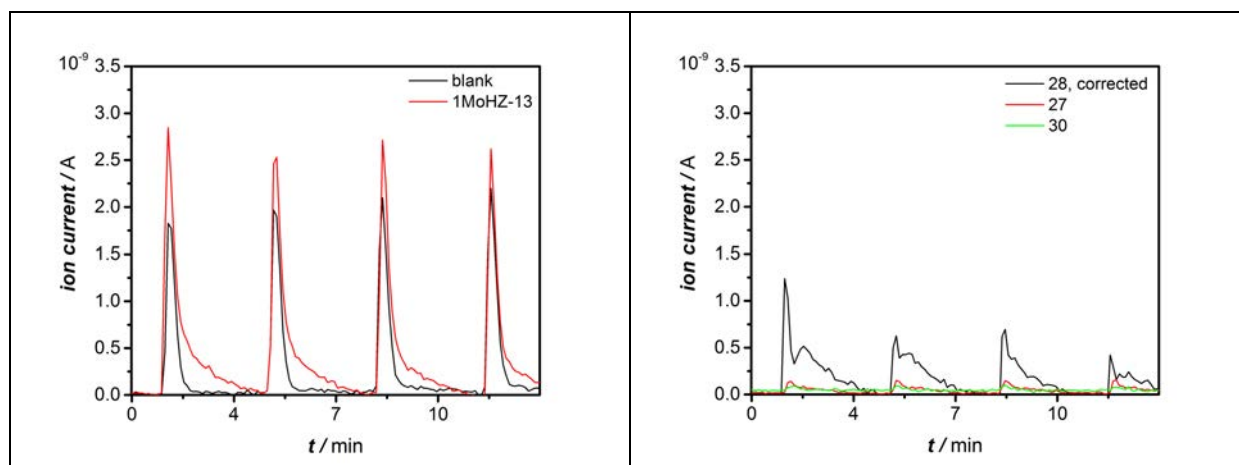


Figure S8: A) Ion current for $m/z = 28$ of a blank measured during consecutive pulsing of 223 μmol of CH₄ at RT to an empty reactor compared with the ion current for $m/z = 28$ during pulse 16-19 over 1MoHZ-13 (see Figure S5). The pressure pulse caused by the injection resulted in an apparent $m/z = 28$ signal B) Signals $m/z = 27, 28$ and 30 corresponding to ethylene and ethane during pulses 16-19 over 1MoHZ-13, where $m/z = 28$ was corrected for the pressure pulse by subtracting the m/z signal measured during the blank experiment.

X-ray Absorption spectroscopy (XAS)

The structural analysis of the Mo/HZSM-5 catalyst was performed *operando* with a pulsing gas set-up at the CRG-FAME UHD beamline (BM16) at the European Synchrotron Radiation Facility (ESRF) in Grenoble.^[6] The XAS cell previously described consists of a vitreous carbon reactor i.d. 4 mm. 100 mg of 2MoHZ-13 catalyst sieved to 250 - 300 μm were loaded into the reactor. The effluent gas composition was monitored on-line by an EcoCat-P portable mass spectrometer (ESS). XANES spectra on the MDA catalyst were recorded either in fluorescence with a Silicon Drift Detector (Vortex-60EX) with a 50 mm² active area (energy resolution: 250 eV) or in transmission mode for the references at the Mo K-edge (20.0 keV).

The CO carburization was performed by heating the fresh sample up to 780 °C (10 °C/min) with a 30 ml/min flow of 2.5% CO in He. In Figure S9, the signals of CO ($m/z = 28$) and CO₂ ($m/z = 44$) are shown in Panel A, while the recorded XANES spectra are shown in Panel B. The sample was left at 780 °C until a negligible amount of CO₂ evolved (~ 11 min). Then, the sample was cooled down to room temperature under CO flow and the reactor was purged with an helium flow (10 ml/min) prior to the CH₄ pulsing experiment.

For the CH₄ pulsing experiments, the 2MoHZ-13 catalyst (either CO carburized or untreated) was first heated under an helium flow (10 ml/min) up to 700 °C with a heating rate of (20 °C/min). Then, 223 μmol CH₄ pulses were introduced into a He flow of 10 ml/min while maintaining a temperature of 700 °C. The signals recorded during CH₄ pulsing for CO, C₂H₄/C₂H₆, CO₂, C₆H₆ and H₂ ($m/z = 28, 27, 44, 78, 2$) as well as CH₄ conversion are shown in Figure S10. Spectra were collected right after each pulse without cooling down and are shown in Figure S11 in Panel A for the CO treated catalyst and in Panel B for untreated catalyst. The spectrum highlighted in pink in Figure S11, Panel B signifies the spectra after the 5th pulse, where Mo sites becomes active to form benzene. This spectrum is very similar to the spectrum taken after the completion of CO carburization. It is clear that the reduction degree is very similar for the two cases, demonstrating that the same active Mo species are formed. Reference spectra for MoO₂, MoO₃, Na₂MoO₄, Mo₂C and Mo-foil are shown in Figure S12 together with a spectrum of 2MoHZ-13 carburized in CO recorded under *in-situ* carburization at 780 °C in fluorescence mode. The spectrum of 2MoHZ-13 carburized in CO is mostly similar to the Mo₂C reference, but the post-edge features differ slightly. Figure S13 shows the EXAFS spectra collected at RT right at the onset of benzene formation when pulsing CH₄ to the He-treated sample and after CO carburization. The Mo₂C reference spectrum is added for comparison. This shows that all main vibrations are in phase with the Mo₂C reference while being much lower in intensity. This is consistent with FT-EXAFS in Figure S14 showing a similar Mo-Mo distance for all three samples, while the intensity of this feature is lower for the samples activated in CO and CH₄ compared to the Mo₂C reference.

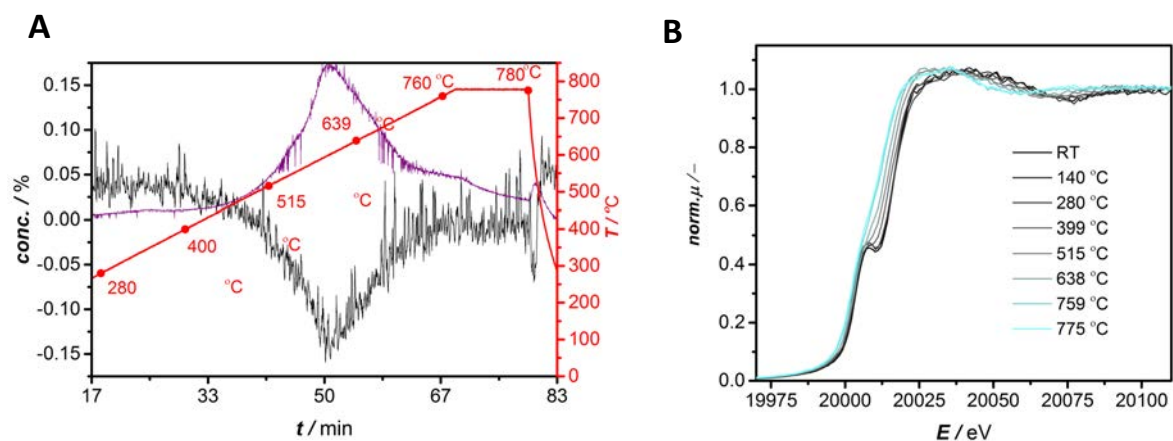


Figure S9: Concentrations of CO ($m/z = 28$, black) and CO₂ ($m/z = 44$, purple) recorded by online-MS analysis during the CO carburization treatment of the 2MoHZ-13 catalyst (Panel A). Highlighted data points in Panel A correspond to the temperatures at which Mo K-edge XANES spectra were recorded (Panel B). Experimental conditions: 100 mg of catalyst were subjected to a 30 ml/min flow of 2.5%CO in He, heating up to 780 °C at 10 °C/min and cooling down after CO₂ evolution ceased to be detected.

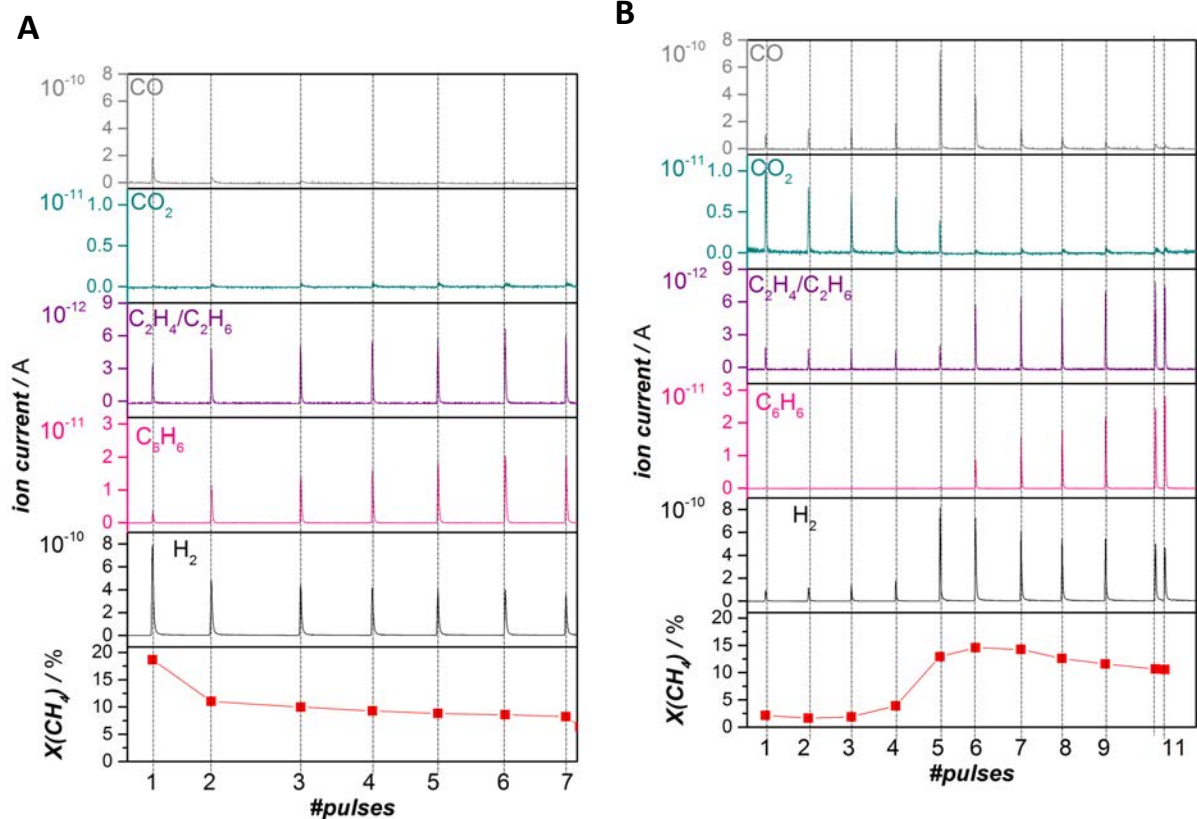


Figure S10: Signals for CO , $\text{C}_2\text{H}_4/\text{C}_2\text{H}_6$, CO_2 , C_6H_6 and H_2 ($m/z = 28, 27, 44, 78, 2$) as well as the CH_4 conversion recorded by online-MS analysis during the CH_4 pulsing for untreated catalyst (Panel A) and CO treated 2MoHZ-13 catalyst (Panel B). Experimental conditions: $223 \mu\text{mol CH}_4$ pulses were introduced into a He flow of 10 ml/min while maintaining a temperature of 700°C . 100 mg of catalyst were used.

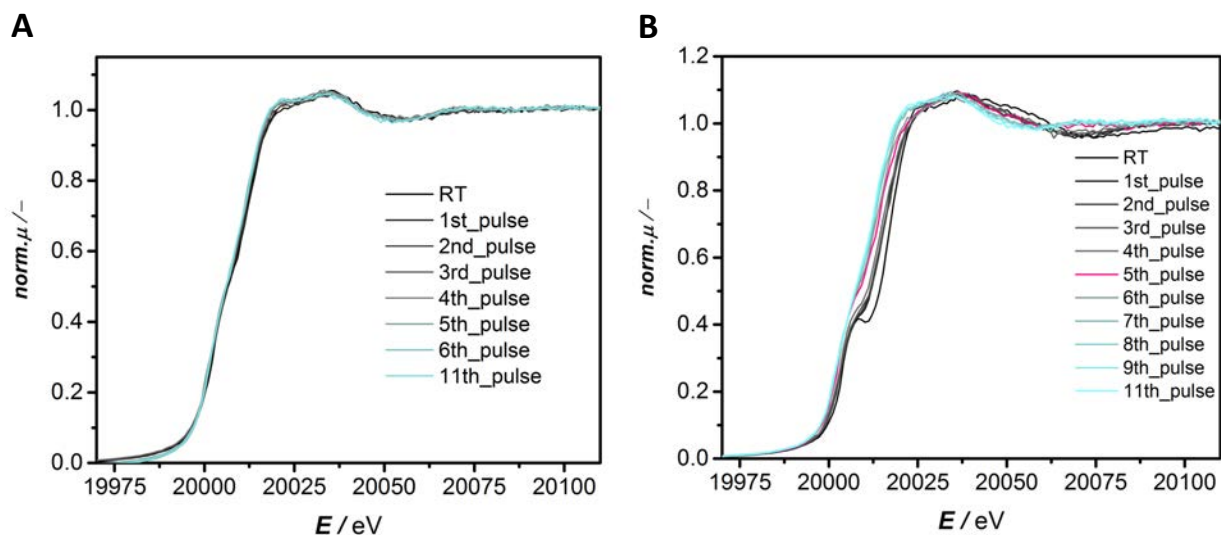


Figure S11: XANES spectra collected at Mo K-edge during CH_4 pulsing at 700°C with a 2MoHZ-13 catalyst pretreated in He (Panel A) and 30 ml/min 2.5%CO in He at 780°C for 1 h (Panel B). Experimental conditions: $223 \mu\text{mol CH}_4$ pulses were introduced into a He flow of 10 ml/min while maintaining a temperature of 700°C . 100 mg of catalyst were used.

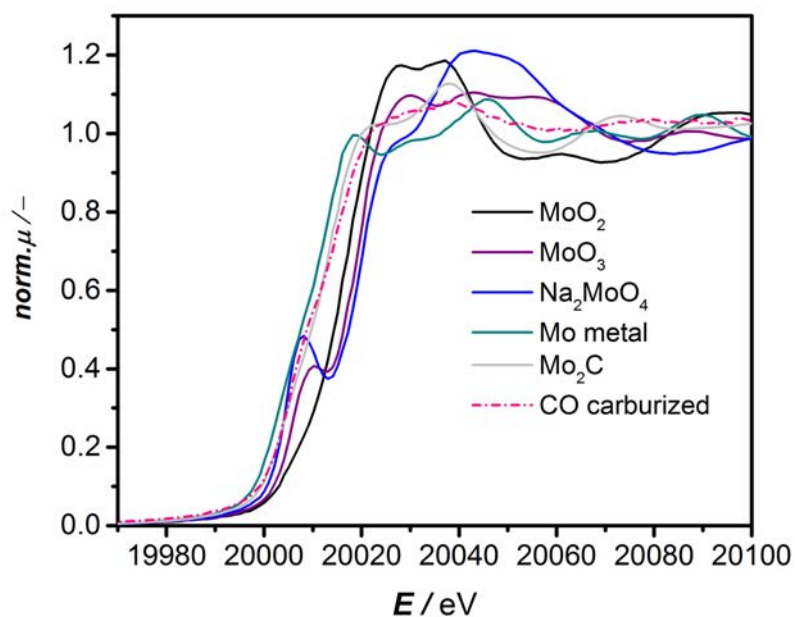


Figure S12: Absorption spectra collected at Mo K-edge for references measured in transmission mode and a 2MoHZ-13 carburized in CO measured in-situ in fluorescence mode.

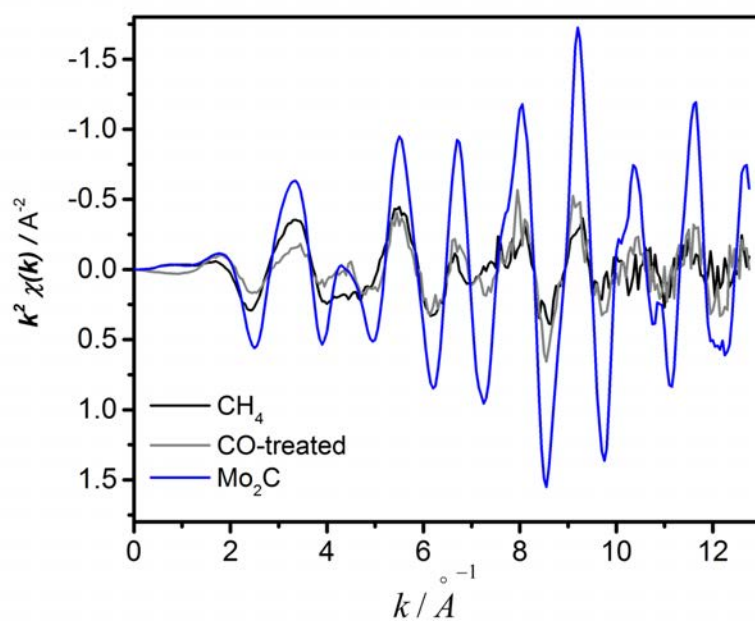


Figure S13: EXAFS spectra collected at Mo K-edge for references measured in transmission mode and a 2MoHZ-13 collected at RT right at the onset of benzene formation when pulsing CH_4 to the He-treated 2MoHZ-13 sample and after CO carburization measured in fluorescence mode.

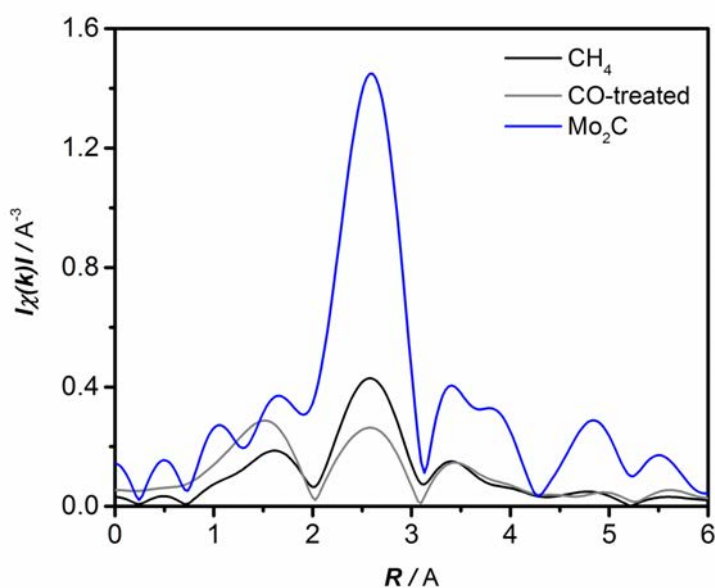


Figure S14: Fourier Transformed EXAFS spectra collected at Mo K-edge for references measured in transmission mode and a 2MoHZ-13 collected at RT right at the onset of benzene formation when pulsing CH_4 to the He-treated 2MoHZ-13 sample and after CO carburization measured in fluorescence mode.

In addition, XANES spectra were measured ex-situ at the Mo K-edge in transmission at the BM26B DUBBLE beamline of the European Synchrotron Radiation Facility (ESRF), Grenoble, France. Those measurements on pelletized samples provide XANES spectra with a better signal to noise ratio compared to spectra measured in the previous *operando* set-up. Prior to measurement, the fresh samples were dehydrated under a flow of N_2 at 400 °C for 16 h. Samples carburized as described in section “CO carburization” were transferred from the carburization setup to the glovebox without exposure to the atmosphere, where they were packed into custom-made holders under inert atmosphere. Figure S15 shows the readouts on the MS during CO carburization at different temperatures. These quasi in-situ results are shown in Figures S16-S17 for the 2MoHZ-13 and 5MoHZ-13 catalysts. The results are comparable to the previous *operando* experiments and confirm a similar carburization state of Mo species obtained by CH_4 pulsing or CO pre-treatment.

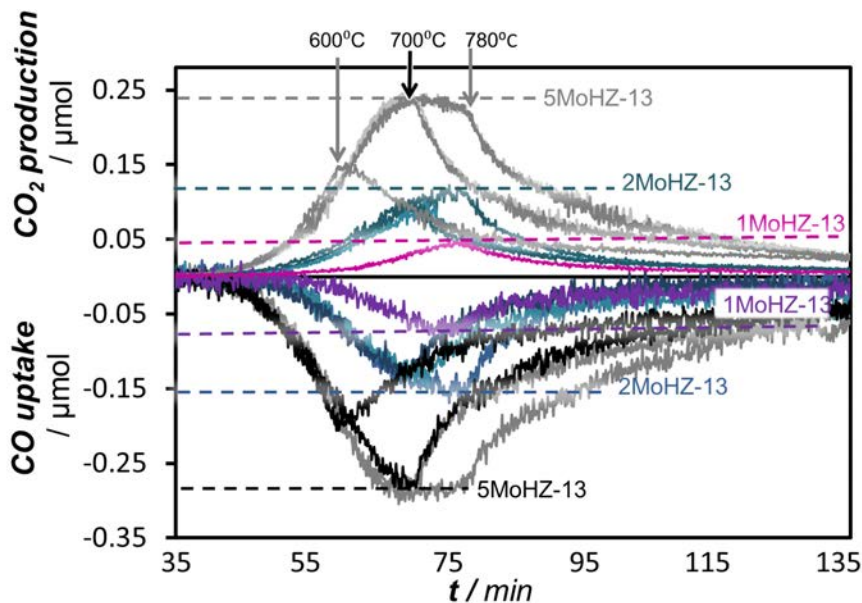


Figure S15: CO₂ evolution (positive scale) and CO consumption (negative scale) upon CO carburization of 2 wt.% and 5 wt.% Mo on HZ-13 with 30 ml/min 2.5% CO in He at 600 °C, 700 °C and 780 °C. Line colors correspond with the sample colors, maximum temperatures applied for the carburization are indicated with arrows at the top.

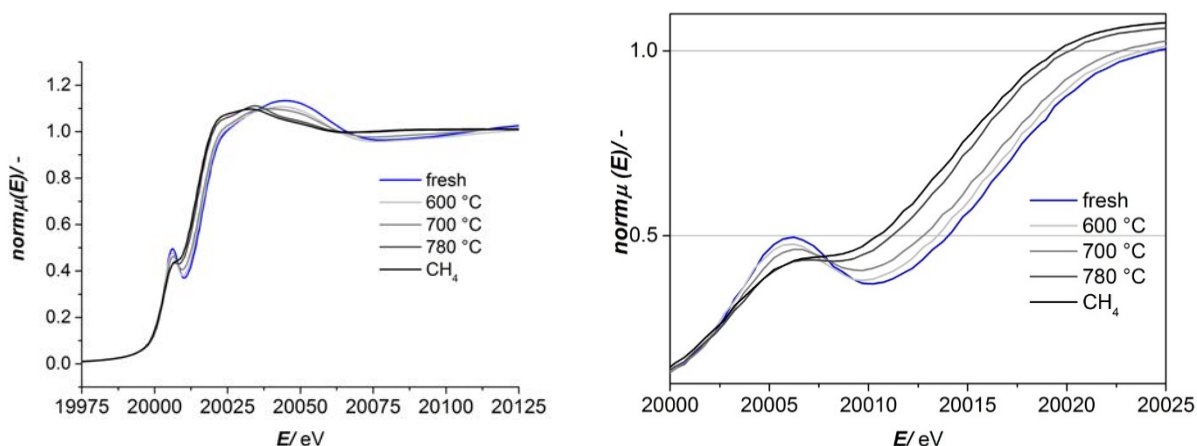


Figure S16: XANES spectra of 2MoHZ-13 collected at Mo K-edge carburized at 600, 700 and 780 °C as described in section “CO carburization” compared to a sample taken from the reaction with methane, which was quenched right at the onset of benzene formation (indicated as “CH₄”) and a sample degassed at 400 °C. All samples were transferred to the glovebox after treatment, where they were packed into XAS sample holders. The right graph presents a zoom-in of the edge.

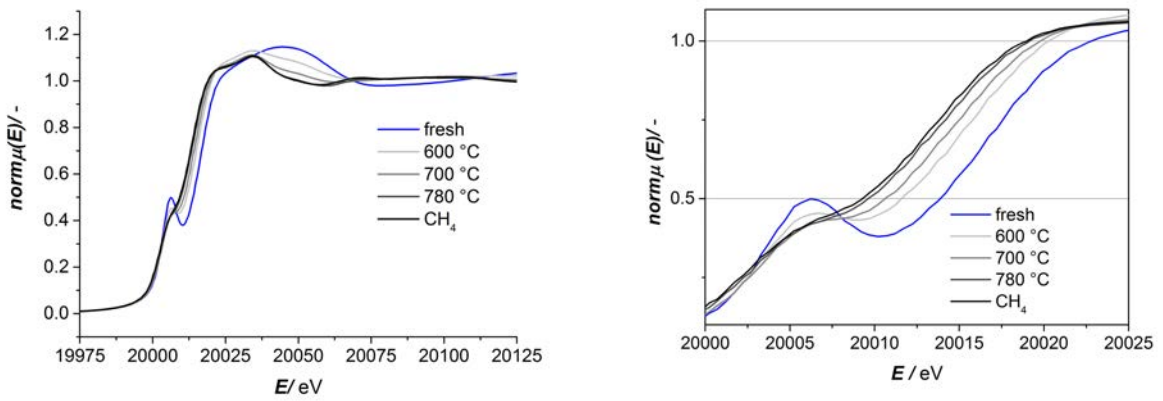


Figure S17: XANES spectra of 5MoHZ-13 collected at Mo K-edge carburized at 600, 700 and 780 °C as described in section “CO carburization” compared to a sample taken from the reaction with methane, which was quenched right at the onset of benzene formation (indicated as “CH₄”) and a sample degassed at 400 °C. All samples were transferred to the glovebox after treatment, where they were packed into XAS sample holders. The right graph presents a zoom-in of the edge.

^{13}C MAS NMR

The samples were prepared as described in section “CO carburization” and transferred from the carburization setup to the glovebox without exposure to the atmosphere. A known amount of sample was filled into zirconia rotors inside the glovebox and tightly closed. 1D ^{13}C MAS NMR spectra were recorded on a Bruker AVANCE III spectrometer operating at resonance frequencies of 100 MHz, and using a conventional double resonance 4 mm CPMAS probe. The spinning frequency was set to 15 kHz. NMR chemical shifts are reported with respect to TMS as the external reference. Spectra were recorded by a spin echo pulse sequence (pulse length 3.4 μs) with four-phase alternation synchronized with the spinning rate for the MAS experiments. The interscan delay was set to 30 s to allow the complete relaxation, and 5,000-30,000 scans were performed. An apodization function (exponential) corresponding to a line broadening of 80 Hz was applied prior to the Fourier transformation. For quantitative analysis, Mo_2C was used as an external reference. Amount of carbon ($\mu\text{mol}\cdot\text{g}^{-1}$) was derived from the deconvoluted Mo_2C spectrum normalized by the amount of scans, weight of the sample and natural abundance of ^{13}C .

Deconvolution of ^{13}C NMR spectra

Carbon amounts obtained from the deconvolution using Gaussian-Lorentzian fitting are summarized in Table S21. Carbon amounts predicted by TPC are about 4 times higher than carbon amounts obtained by deconvolution of the ^{13}C NMR spectra. The fact that this factor is the same for all three loadings of Mo suggests a systematic error in the deconvolution of ^{13}C NMR. This can be due to a slight re-oxidation of the active site, although exposure to oxygen was limited as much as possible.

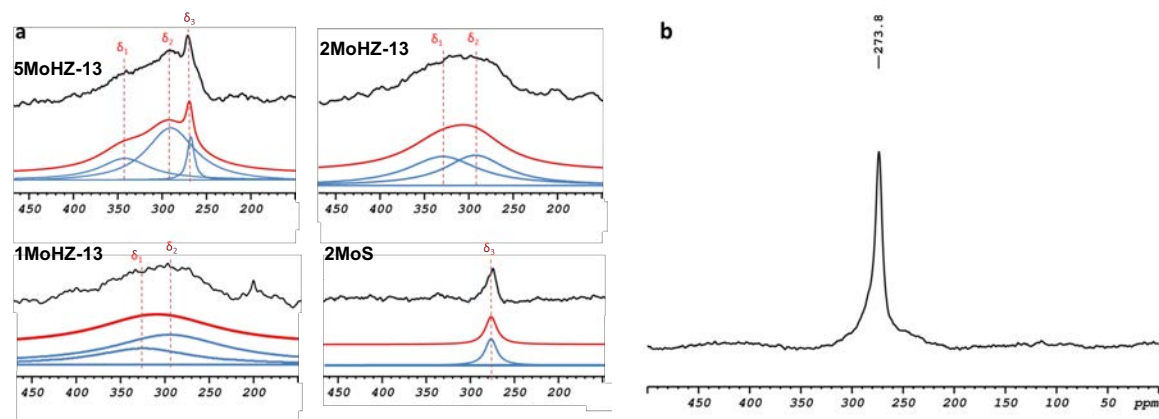


Figure S18: a. Deconvolution results of ^{13}C MAS NMR spectra of MoHZ-13 after ^{13}CO carburization using Lorentzian-Gaussian fitting. b. Spectra collected with Mo_2C reference.

Table S2: ^{13}C MAS NMR chemical shifts deconvolution and quantification of carbidic species obtained after ^{13}CO carburization of Mo loaded HZ-13 and silicalite-1 compared to carbon content determined from TPC.

Catalyst	δ_1 (338 ppm)		δ_2 (290 ppm)		δ_3 (270 ppm)		$\sum\delta$	Carbon content from TPC
	% ^a	$\mu\text{mol} \cdot \text{g}^{-1b}$	% ^a	$\mu\text{mol} \cdot \text{g}^{-1b}$	% ^a	$\mu\text{mol} \cdot \text{g}^{-1b}$		
1MoHZ-13	22	7.0	78	25.0	0	0.0	32.0	137.0
2MoHZ-13	53	28.3	47	25.0	0	0.0	53.3	201.9 ^d
5MoHZ-13	36	28.3	57	44.7	7	5.5	78.5	308.3
2MoS	0	0.0	0	0.0	100	27.5	27.5	

^a Relative concentration of carbidic species (%) obtained from deconvolution using mixed Gaussian-Lorentzian fitting.
^b Calculated using Mo_2C as external standard.
^c calculated from curves in Figure S4, see section 'CO carburization-Quantification' for details on calculation
^d obtained by averaging 3 experiments

Temperature Programmed Oxidation (TPO)

Temperature Programmed Oxidation (TPO) was performed on a custom-made setup, where a 30 ml/min flow of 5% O_2 in He was continuously fed to the reactor. Effluent gasses were analyzed by a quadrupole mass spectrometer (Balzers) connected on-line with the reactor. Mass Spectra were recorded in multiple ion detection (MID) mode using a channeltron detector. Quantification of CO and CO_2 was achieved by calibrating signals with calcium oxalate.^[2] Signals were normalized with the signal of He and the fragmentation contribution of CO_2 $m/z = 44$ was subtracted from $m/z = 28$. The catalyst was pretreated by TPC.

Figure S19 shows the evolution of CO (dashed lines) and CO_2 (solid lines) evolution during TPO of 1, 2 and 5MoHZ-13 previously carburized in CO at 780 °C. Mainly CO_2 evolves while CO production is negligible. At least three different CO_2 production contributions can be observed, corresponding to different Mo (oxy-)carbides, well in line with the three species δ_1 , δ_2 and δ_3 observed in ^{13}C NMR (see section " ^{13}C MAS NMR"). The first peak between 84 °C and 142 °C likely corresponds to small Mo oxycarbide species inside the pores of the zeolite, which are easy to oxidize, since this is most significant peak for 1MoHZ-13 and it is known that Mo only exists as mono- or dimeric species in that 1MoHZ-13.^[7] This amount is about the same for all three loadings. The second peak between 281 °C and 251 °C increases with Mo-loading attributed to slightly bigger species still inside the pores of the zeolite corresponding to δ_2 from ^{13}C NMR. The third peak at 377 °C is only observed for 5MoHZ-13, which is small compared to the other two peaks for 5MoHZ-13, and matching the results from ^{13}C NMR well, where δ_3 only makes up 4% of all the carbon in that catalyst. This peak is attributed to Mo_2C nanoparticles at the external surface of the zeolite.

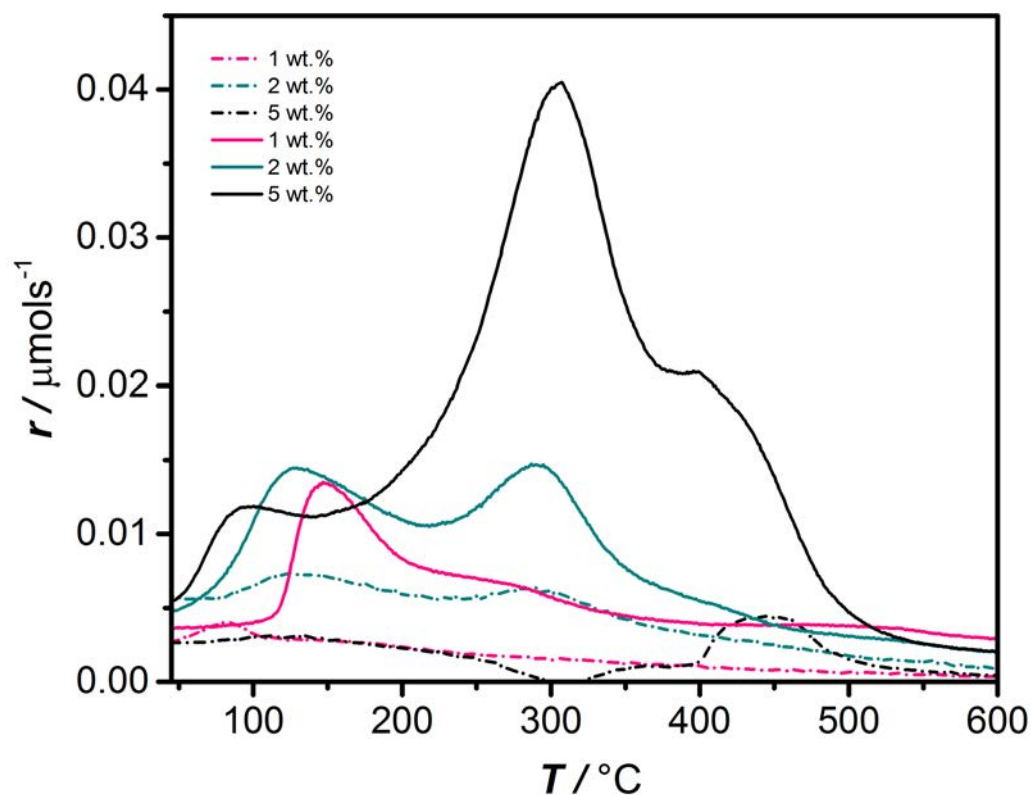


Figure S19: CO (dashed lines) and CO₂ (solid lines) evolution for 1, 2 and 5MoHZ-13, previously carburized in CO during TPO with 30 ml/min of 5% O₂ in He heating to 770 °C with 10 °C/min.

Table S3: Carbon content as determined from Figure S4 and Figure S19 for 1, 2 and 5MoHZ-13.

Catalyst	Carbon content from TPC	Carbon content from TPO	% difference
	C/Mo	C/Mo	%
1MoHZ-13	1.3	1.0	25
2MoHZ-13	1.1	1.0	13
5MoHZ-13	0.6	0.4	27

Activity Relationships

Figures S20-S21 relate maximum conversion of methane to total carbon content in $\mu\text{mol/g}$ as determined by deconvolution of ^{13}C NMR (section “ ^{13}C NMR”).

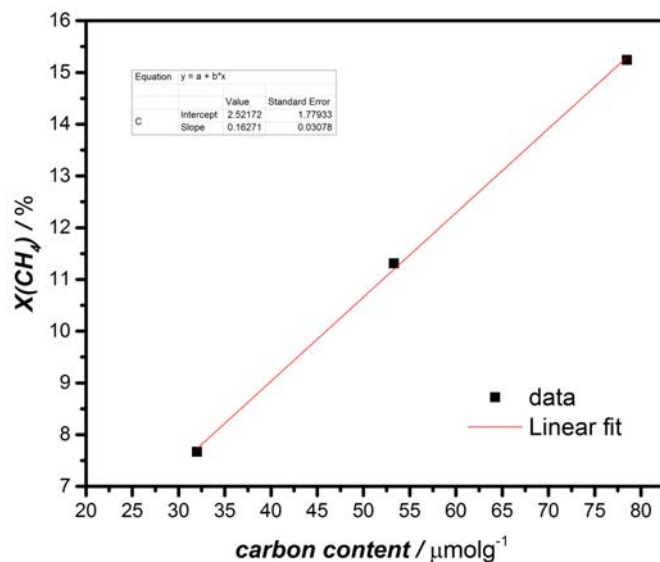


Figure S20: Maximum conversion of methane plotted against carbon content determined by quantification of ^{13}C NMR results for 1MoHZ-13, 2MoHZ-13 and 5MoHZ-13.

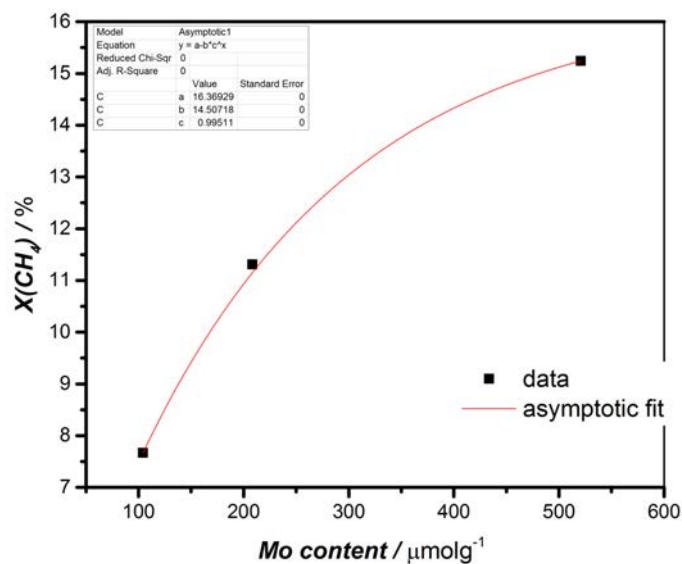


Figure S21: Maximum methane conversion plotted against Mo content for 1MoHZ-13, 2MoHZ-13 and 5MoHZ-13.

Catalytic performance

Catalytic testing was performed in a quartz reactor tube with an inner diameter of 6 mm, using 500 mg catalyst pelletized to pellets of 212 to 425 μm . A weight hourly space velocity (WHSV) of 1.21 h^{-1} (based only on methane flow) and a reaction temperature of $700 \text{ }^\circ\text{C}$ was applied in all tests. Product analysis was achieved on an Interscience Trace GC with a TCD and two FIDs. A mixture 5% N_2 in CH_4 was fed to the reactor, where N_2 was used as an internal standard. The reactor was brought to reaction temperature under the same flow with a heating rate of $10 \text{ }^\circ\text{C}/\text{min}$. Although trace amount of many products were detected in the calculations only the major products were considered (hydrogen, ethylene, ethane, propylene, benzene, toluene, xylenes and naphthalene).

Product yields were calculated according to Equation 18:

$$Y_{\text{product}}[\text{mol}\%] = \frac{F_{C_iH_j}}{F_{CH_4, \text{in}}} * i * 100\% \quad \text{Equation 18}$$

Conversion of methane is shown in Figure S22 for 1MoHZ-13, 2MoHZ-13 and 5MoHZ-13. While benzene yields and naphthalene yields are shown in Figure S23 and Figure S24 respectively.

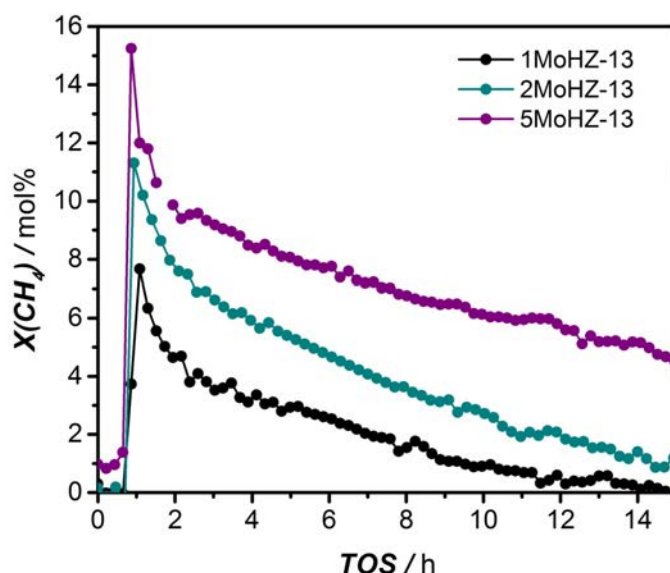


Figure S22: CH_4 conversion for 1MoHZ-13, 2MoHZ-13 and 5MoHZ-13 tested at $700 \text{ }^\circ\text{C}$ with 500 mg catalyst and a $\text{WHSV} = 1.21 \text{ h}^{-1}$.

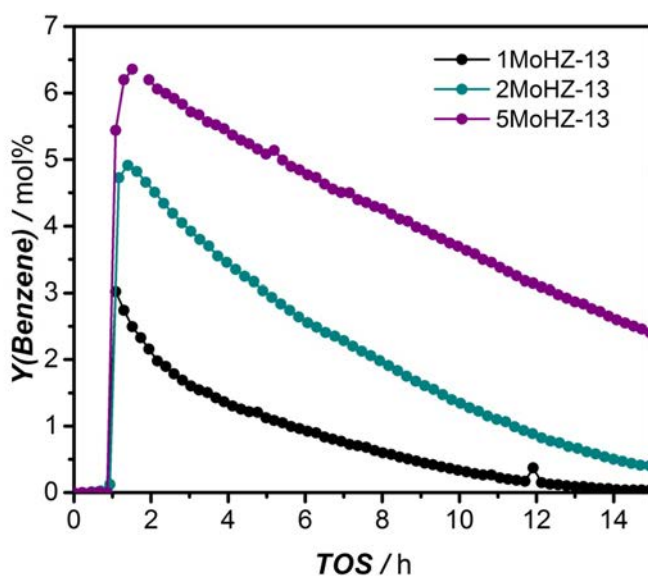


Figure S23: Benzene yields for 1MoHZ-13, 2MoHZ-13 and 5MoHZ-13 tested at 700 °C with 500 mg catalyst and a WHSV = 1.21 h⁻¹.

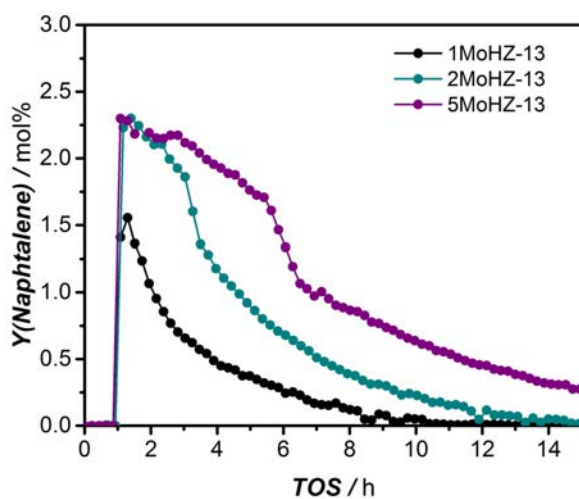
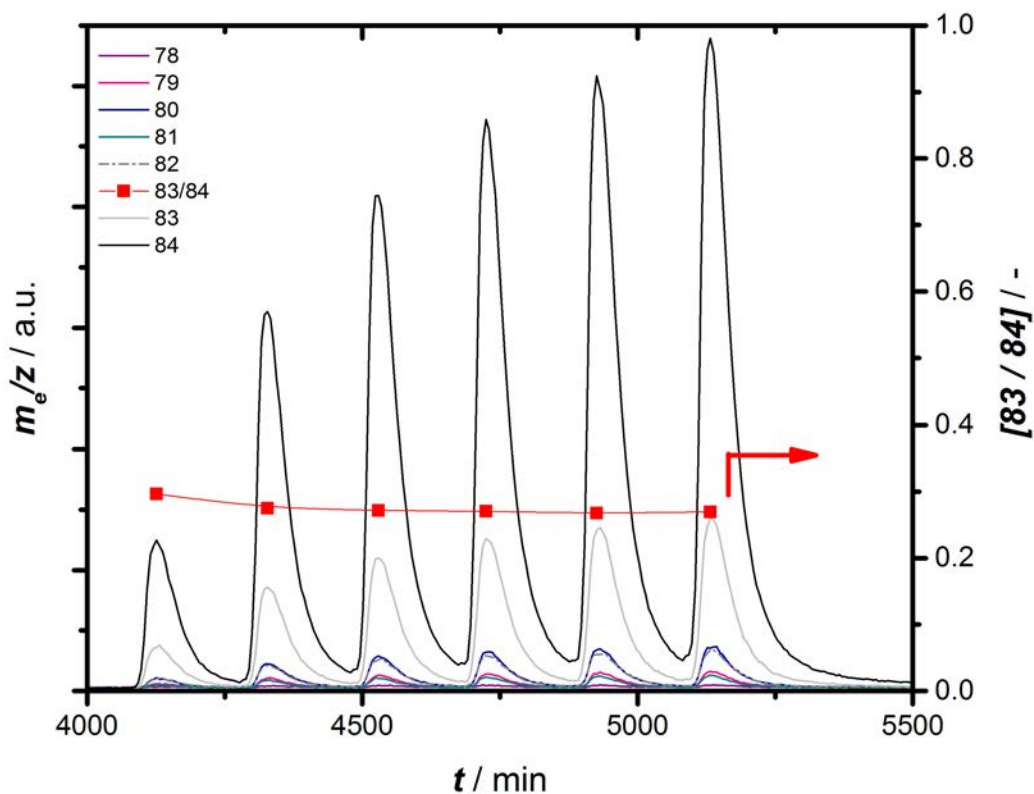


Figure S24: Naphthalene yields for 1MoHZ-13, 2MoHZ-13 and 5MoHZ-13 tested at 700 °C with 500 mg catalyst and a WHSV = 1.21 h⁻¹.

CH₄ pulsing using labelled molecules

Benzene control experiments

A



B

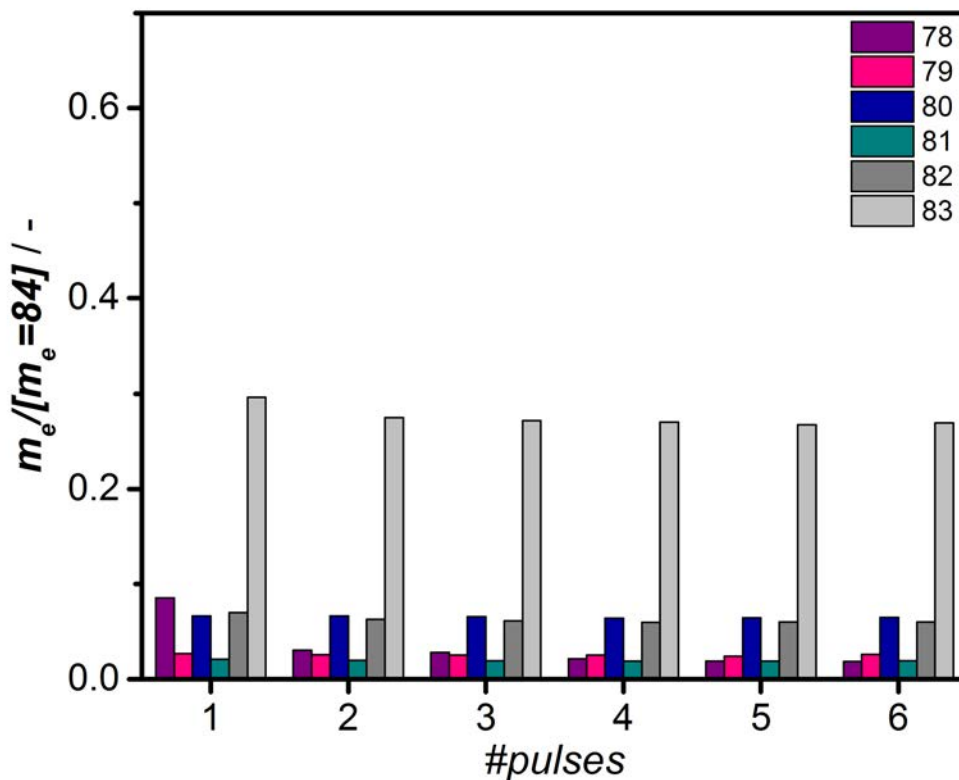
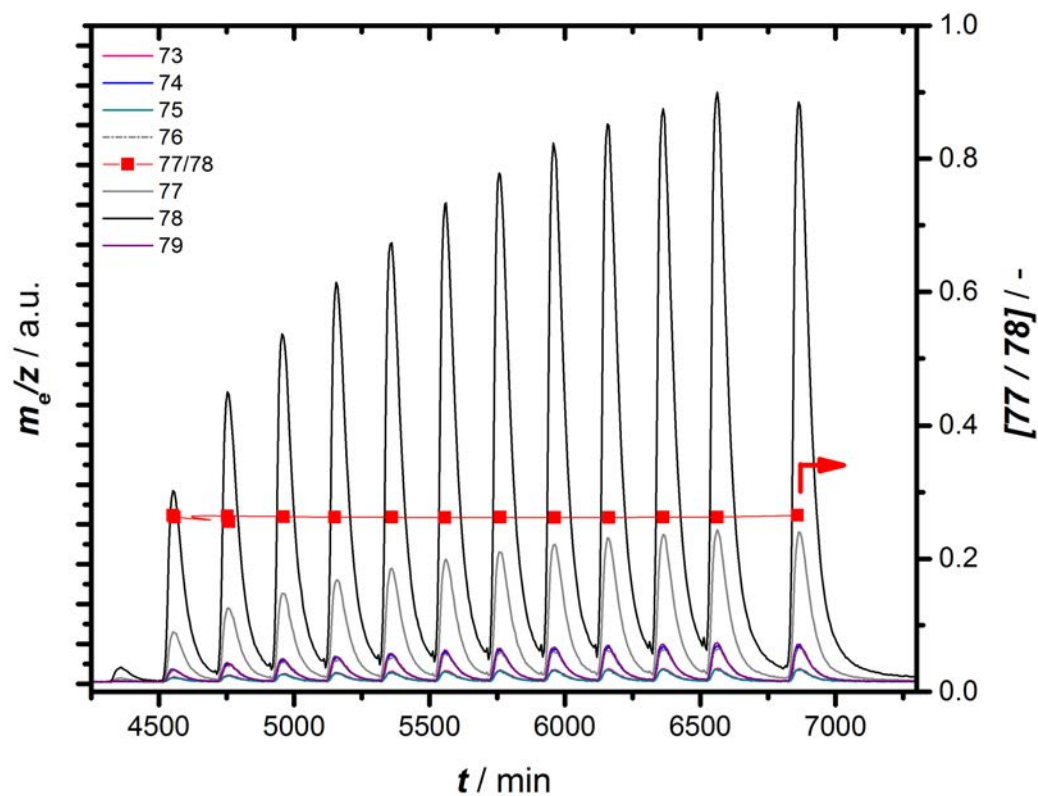


Figure S25: Development of MS readouts for several fragments representative of ¹³C₆H₆ during consecutive pulsing of ¹³CH₄ to 300 mg of 2MoHZ-13 carburized with 30 ml/min of 2.5% ¹³CO in He at 780 °C for 1 h (Panel A). Panel B shows the integrated peak areas per pulse normalized by m/z = 84.

A



B

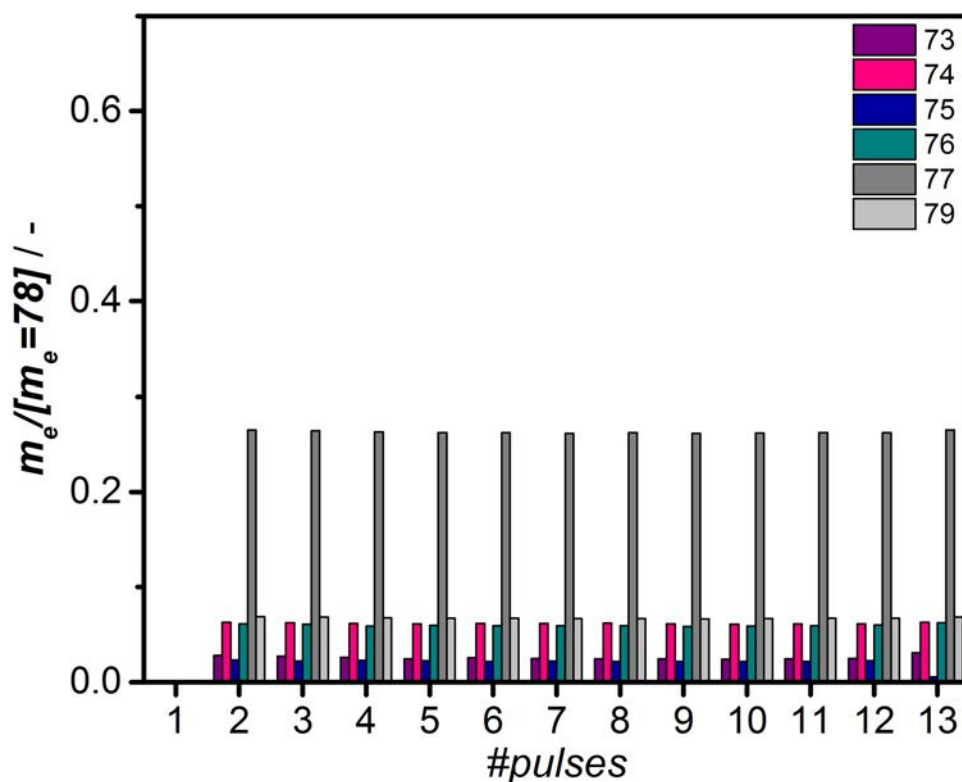


Figure S26: Development of MS readouts for several fragments representative of $^{12}\text{C}_6\text{H}_6$ during consecutive pulsing of $^{12}\text{CH}_4$ to 300 mg of 2MoHZ-13 carburized with 30 ml/min of 2.5% ^{12}CO in He at 780 °C for 1 h (Panel A). Panel B shows the integrated peak areas per pulse normalized by $m_e/z = 78$.

Ethylene and ethane

To investigate the incorporation of carbon from the active site into ethylene and ethane, masses 26 to 30 were recorded on the MS. Figure S27 shows both the control experiment (Panel A) and the experiment in which labelled ^{13}CO was used (Panel B). For the control experiment 300 mg of 2MoHZ-13 were treated with 30 ml/min of 2.5% $^{12}\text{C}^{18}\text{O}$ in He at 780 °C for 1h. After this pretreatment both samples were subjected to CH_4 pulsing. Comparing Panel A and B, it becomes clear that the intensity of m/z 29 is much higher in Panel B due to the presence of $^{13}\text{C}^{12}\text{CH}_4$, showing that one carbon in this molecule originates from the active site.

More information can be obtained, because of the use of CO with labelled oxygen, $^{12}\text{C}^{18}\text{O}$. It helped to determine how much oxygen of the as-synthesized catalyst is exchanged during the CO treatment (Figure S3). This leads to the conclusion that all oxygen staying behind on the catalyst should be labelled ^{18}O . Therefore, most of the CO that is released during the initial pulses of CH_4 , should be C^{18}O with $m/z = 30$. In addition, in Panel A of Figure S27 mass 30 is slowly decreasing with each pulse, while mass 28 stays constant starting from pulse 1. Both of these observations lead to the conclusion that mass 28 arises from ethylene in this case. Since the level of $m/z = 28$ in Panel B follows the same trend and intensity as $m/z = 28+30$ in Panel A, none of $m/z = 29$ seems to stem from ^{13}CO , because the amount of CO produced should be the same in both experiments.

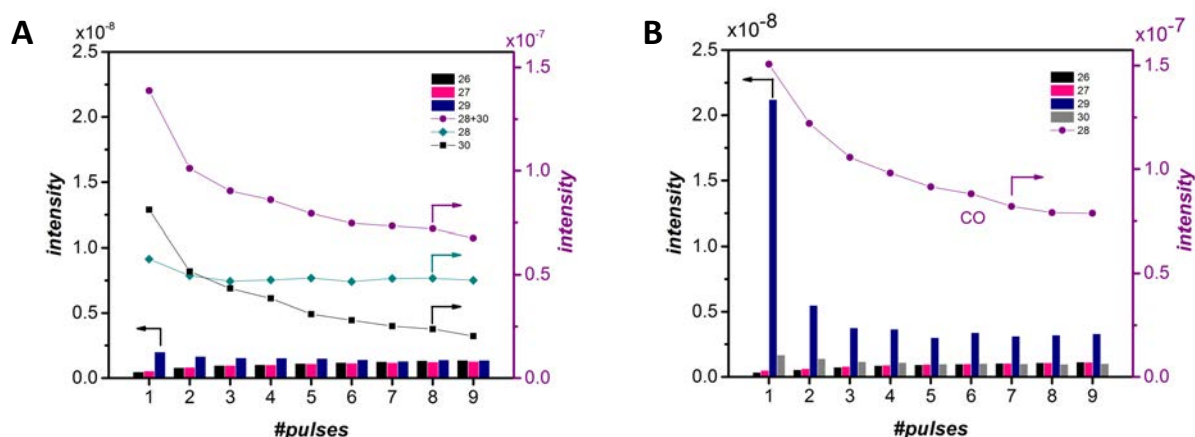


Figure S27: Integrated peak areas per pulse for MS readouts for masses 26 to 30 during consecutive pulsing of $^{12}\text{CH}_4$ at 700 °C to 2MoHZ-13 carburized with 30 ml/min with 2.5% of either $^{12}\text{C}^{18}\text{O}$ (Panel A) or ^{13}CO (Panel B) in He at 780 °C for 1 h.

Gas chromatography-mass spectrometry (GC-MS) analysis of the collected liquid products

To further confirm the results for the online-MS analysis of the products, the liquid products were collected at the outlet by bubbling the effluent gasses through ethylacetate. The collected samples were analysed on a Shimadzu GCMS-QP2010S with a split of 25, an injector temperature of 250 °C and a VF CPsil-5 25mx0.25mmx0.4 µm column. The temperature program consisted of a 5 min hold at 50 °C and then a ramp rate of 70 °C/min to ramp to 325 °C and another hold for 3 min. The MS was operated with the ion source(EI) at 200 °C and the interface at 250 °C and masses between 40 and 600 mu were measured with 0.5 sec per spectrum and a solvent cut time of 1.7 min. Collected samples were compared to a reference of unlabelled benzene.

In Figure S28, a sample collected after the first 4 pulses of $^{13}\text{CH}_4$ to 300 mg of 2MoHZ-13 carburized with 30 ml/min of 2.5% ^{12}CO in He at 780 °C for 1 h are compared to a reference. As also observed with online MS analysis mass 83 is much higher than the fragment at 77 for C_6H_5 of the reference. Figure S29 shows the results of the reverse experiment where carburization was performed with ^{13}CO and pulsing with $^{12}\text{CH}_4$, while keeping all other conditions the same. The sample collected during the first 3 pulses shows a much higher intensity for mass 79, this mass represents $^{13}\text{C}^{12}\text{C}_5\text{H}_6$. For the reference this mass corresponds to the natural abundance of the isotope. It is clear from Figure S29 that the intensity for this mass exceeds the value for natural abundance in benzene of $6 \times 1.1\%$ for the sample collected after the first 3 pulses. This value is lower for the sample collected during pulse 4 to 8, but is still above the value corresponding to natural abundance.

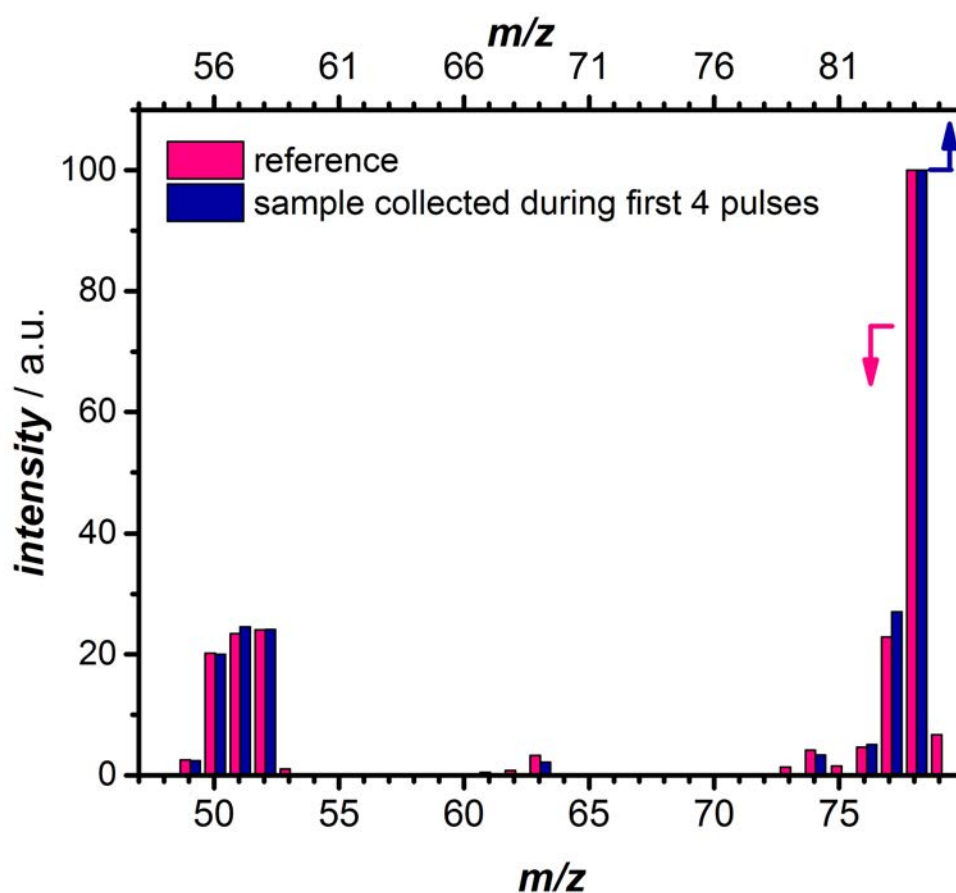


Figure S28: Fragmentation pattern obtained from GC-MS analysis of benzene collected during the first 4 pulses of $^{13}\text{CH}_4$ to 300 mg of 2MoHZ-13 carburized with 30 ml/min of 2.5% ^{12}CO in He at 780 °C for 1 h compared to unlabeled benzene as a reference. The top axis refers to the collected sample, while the bottom axis refers to the non-enriched reference.

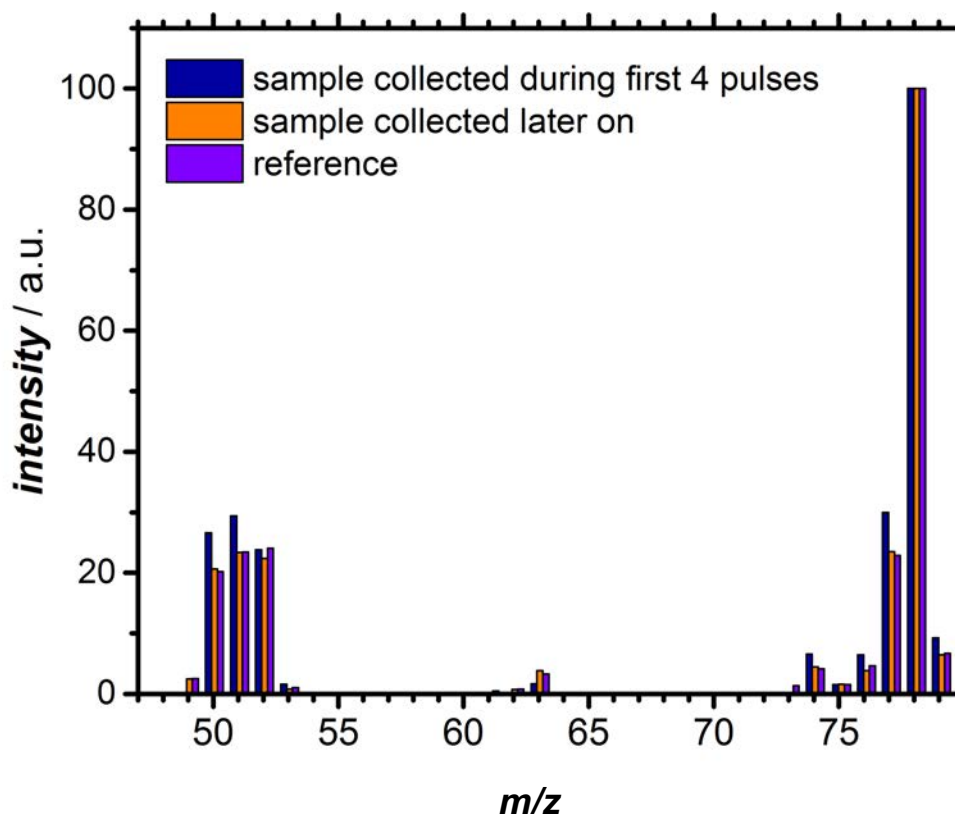


Figure S29: Fragmentation pattern obtained from GC-MS analysis of benzene collected during the first 3 pulses of $^{12}\text{CH}_4$ to 300 mg of 2MoHZ-13 carburized with 30 ml/min of 2.5% ^{13}CO in He at 780 °C for 1 h compared to a sample collected during pulse 4-8 and a non-enriched benzene as a reference.

N_2 Adsorption

N_2 Adsorption was performed on a TriStar II 3020 Version 3.02 (Micromeritics) at liquid nitrogen temperature, $T = -196$ °C. The equilibration interval amounted to 12 s. Before running the adsorption, the catalyst was outgassed under a flow of N_2 at 350 °C for 16 h. The Brunauer-Emmet-Teller theory was applied to determine the BET area of the catalyst and the t -plot method to determine the micropore volume. The isotherm obtained for HZ-13 calcined at 550 °C for 7 h, heating with 2 °C/min, is shown in Figure S30. The micropore volume was determined to be 0.132 m^3/g and the BET area 350 m^2/g .

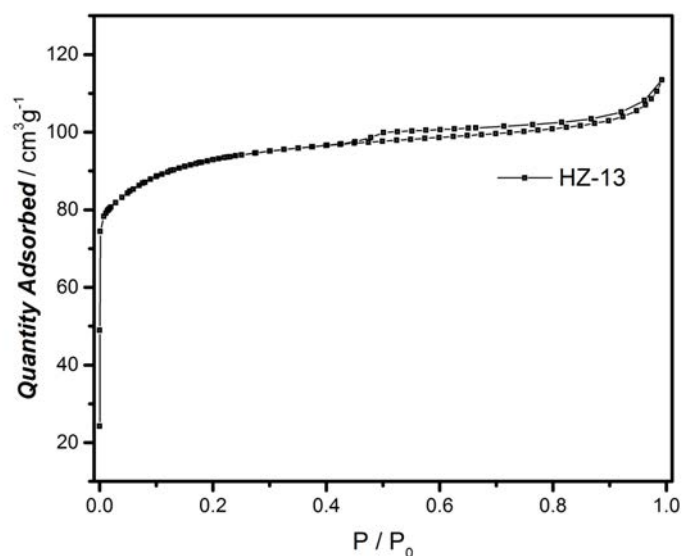


Figure S30: N₂ isotherm measured at liquid N₂ temperature on HZ-13, calcined at 550 °C for 7 h, heating with 2 °C/min.

PXRD

For Powder X-Ray Diffraction (PXRD), a Bruker D8 Advance diffractometer was used operating in Bragg-Brentano geometry using Co K α radiation ($\lambda = 0.179$ nm) and a Lynxeye position sensitive detector to collect data in the range of 2θ from 5° to 50° with a scan-speed of 0.2°s⁻¹ and a sample rotation of 30 rpm. Figure S31 shows the diffraction pattern of HZ-13 calcined at 550 °C for 7 h, heating with 2 °C/min. The zeolite shows the typical diffraction pattern of a zeolite with MFI topology.

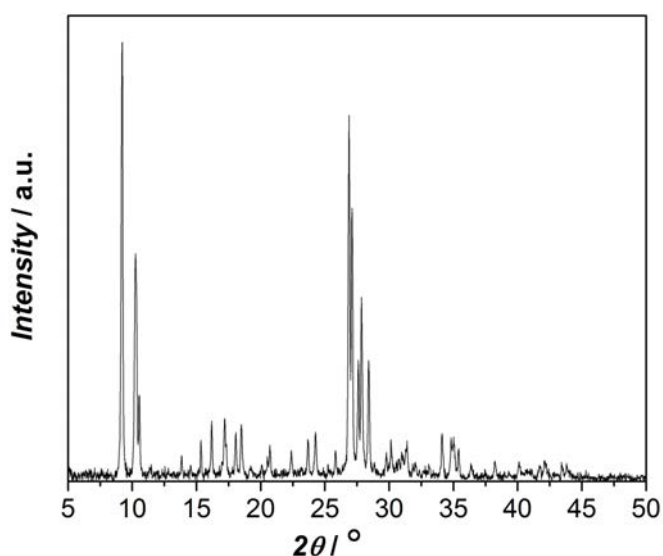


Figure S31: PXRD pattern of HZ-13, calcined at 550 °C for 7 h, heating with 2 °C/min.

References

- [1] N. Kosinov, V. G. P. Sripathi, E. J. M. Hensen, *Microporous and Mesoporous Materials* **2014**, *194*, 24-30.
- [2] J. Wang, B. McEnaney, *Thermochimica Acta* **1991**, *190*, 143-153.
- [3] T. V. Voskoboinikov, H. Y. Chen, W. M. H. Sachtler, *Journal of Molecular Catalysis A: Chemical* **2000**, *155*, 155-168.
- [4] J. Valyon, W. K. Hall, *Journal of Catalysis* **1993**, *143*, 520-532.
- [5] aU. S. S. o. Commerce, *Vol. 2018*, The National Institute of Standards and Technology **2017**;
bU. S. S. o. Commerce, *Vol. 2018*, The National Institute of Standards and Technology **2017**.
- [6] B. AlSabban, L. Falivene, S. M. Kozlov, A. Aguilar-Tapia, S. Ould-Chikh, J.-L. Hazemann, L. Cavallo, J.-M. Basset, K. Takanebe, *Applied Catalysis B: Environmental* **2017**, *213*, 177-189.
- [7] N. Kosinov, A. S. G. Wijkema, E. Uslamin, R. Rohling, F. J. A. G. Coumans, B. Mezari, A. Parastayev, A. S. Poryvaev, M. V. Fedin, E. A. Pidko, E. J. M. Hensen, *Angewandte Chemie* **2018**, *57*, 1016-1020.